Article:
Tang, X., Xu, J., Wang, R. et al. (2026) Drivers of cross-boundary land use and cover change in a megacity region: Evidence from the Guangdong–Hong Kong–Macao Greater Bay area. Sustainability, 18 (1). 470. ISSN: 2071-1050

https://doi.org/10.3390/su18010470

sustainability

MDPI

Article

Drivers of Cross-Boundary Land Use and Cover Change in a Megacity Region: Evidence from the Guangdong–Hong Kong–Macao Greater Bay Area

Xiao Tang [1,2,3,4], Jiang Xu [3], Rong Wang [5], Jing Victor Li [3], Lin Jiang [1] and Clyde Zhengdao Li [1,*]

[1] Department of Construction Management and Real Estate, Shenzhen University, Shenzhen 518052, China
[2] Department of Urban Studies and Planning, University of Sheffield, Sheffield S10 2TN, UK
[3] Department of Geography and Resource Management, The Chinese University of Hong Kong, Hong Kong; victorli@cuhk.edu.hk (J.V.L.)
[4] Department of Real Estate and Urban Economics, University of Manchester, Manchester M13 9PL, UK
[5] School of Civil Engineering and Built Environment, Liverpool John Moores University, Liverpool L3 3AF, UK
* Correspondence: clyde.zhengdao.li@szu.edu.cn

Abstract

Megacity regions mark a transformative phase of urbanisation, in which interconnected cities undergo land-use and land-cover change (LUCC) that extends beyond administrative boundaries. However, the drivers of cross-boundary LUCC remain insufficiently examined, particularly before the top-down regional integration. The Guangdong–Hong Kong–Macao Greater Bay Area (GBA) provides a clear empirical case, having experienced cross-boundary LUCC prior to its formal designation as a megacity region in 2018. This study builds a Landsat-derived LUCC and driver dataset for the GBA. Global and local spatial autocorrelation (Moran's I and LISA) are used to characterise spatial structure and clustering, and geographically weighted regression identifies the socio-economic and environmental determinants of built-up expansion over 1980–2018, spanning the pre-reform decade and the post-1990 land-transfer era. Findings reveal that: (1) LUCC in the GBA already exhibited a cross-border, spatially networked expansion pattern before formal regional integration policies at the national level, with built-up area growth extending beyond core cities into decentralised urban nodes. Two prominent cross-border cores and one cross-administrative core emerged, suggesting that regional integration was co-led by market forces and local governments before an institutional framework was established. (2) Although the GBA showed a clear trend towards integrated development, urban expansion was highly uneven. Such spatial disparities were mainly driven by varying socioeconomic and natural factors, including gross domestic product, population growth, real estate investment, water resource proximity, and infrastructure development. These findings enhance understanding of megacity-region dynamics and offer insights from the GBA for cross-border urbanisation and sustainable spatial governance.

Keywords: megacity region; land use; land cover; land use and cover change; remote sensing; spatial structure formation; Guangdong–Hong Kong–Macao Greater Bay Area; informal regionalism

Academic Editor: Ana Cláudia Teodoro

Received: 1 October 2025
Revised: 19 November 2025
Accepted: 25 December 2025
Published: 2 January 2026

1. Introduction

In recent years, as urbanisation accelerates, a new form of global urbanisation called "megacity regions" has emerged, characterised by interconnected cities experiencing land

use and cover change (LUCC) beyond traditional administrative boundaries [1,2]. Despite many countries acknowledging the competitive advantages of megacity regions in the global urban system, these regions often face spatial governance challenges due to institutional fragmentation [3]. Given that land serves as a fundamental carrier of human activities and urban development, through formal integration policies coordinating regional LUCC is regarded as an effective approach to governing the spatial structure of megacity regions [4]. Building on this, existing studies have emphasised the pivotal role of formal integration policies in shaping megacity region spatial structures by coordinating regional LUCC [5,6]. Specifically, the formal integration policies would involve establishing clear guidelines and procedures when integrating data and models related to LUCC into decision-making processes, aiming to promote spatial structures of the megacity region that are coordinated and integrated [1,2]. However, despite the growing recognition of megacity regions as spaces of cross-boundary urbanisation, promoting land development in border-adjacent areas is recognised as a core objective of metropolitan spatial integration, and the driving forces of LUCC across administrative boundaries remain underexplored, particularly before the implementation of top-down formal regional integration policies. Measuring the evolutionary phase preceding formal integration is essential for accurately understanding the bottom-up mechanisms and actual growth trajectories of megacity regions, which help support more efficient resource allocation and enhance the effectiveness of policy interventions [3].

The expansion of a built-up area (BUA) represents the most typical LUCC form in megacity regions [1,2]. LUCC research aims to explore changes in the Earth's surface caused by natural processes and human activities. It is an important agenda item in the 2030 United Nations Sustainable Development Goals [7,8]. Since the rise of megacities in the 1960s–1970s, LUCC studies have increasingly focused on urban areas, where the rapid expansion of built-up land presents significant sustainability challenges [9]. LUCC research provides a quantitative approach and comprehensive global datasets for tracing the development of urban spatial evolution [10,11]. This approach is particularly advantageous for analysing the spatial evolution and integration processes within megacity regions, especially in contexts where formal regional integration frameworks are absent [4].

In China, formal regional integration policies are implemented in a top-down approach under the supervision of the central government [3]. The GBA, designated as a megacity region in China, comprising eleven cities [nine mainland cities and two special administrative regions (Hong Kong and Macau)], since 2018 has undergone rapid integration and development. State-led formal integration policies have achieved notable success in promoting cross-border urbanisation and spatial integration in the Guangdong–Hong Kong–Macao Greater Bay Area (GBA) by coordinating LUCC, thereby optimising regional spatial structures and enhancing the coordination of urban functional divisions [6]. Today, the GBA is recognised as the fourth-largest megacity region globally, following New York, San Francisco, and Tokyo Bay Areas.

The success of spatial coordination of the Greater Bay Area (GBA) was not achieved instantaneously. Prior to the centralised coordination and integration stage, the GBA underwent a fragmentation phase of evolution driven predominantly by local governments and market forces. During this period, municipal governments enjoyed substantial autonomy in economic governance [12]. The fiscal decentralisation reforms of the 1990s incentivised local authorities to adopt entrepreneurial strategies, accelerating land development and attracting investment through competitive infrastructure expansion. Particularly noteworthy was the land-mark land reform of 1990, which for the first time authorised local governments in mainland China to transfer state-owned urban land through market mechanisms. This significantly boosted demand for urban built-up land, driving rapid built-up

area expansion throughout the GBA [12]. However, this model also intensified spatial and regulatory fragmentation, as municipal governments prioritised local interests over regional coordination [10,12,13]. Furthermore, under the "one country, two systems" framework, the GBA faced additional complexities due to cross-border governance challenges. Given the dynamic adjustments to governance frameworks experienced during its spatial formation, the GBA provides a critical empirical case study for researching how LUCC affects the spatial structure of megacity regions in the absence of state-led integration policy.

Thus, this paper aims to provide a comprehensive understanding of the drivers of LUCC across boundaries within megacity regions, prior to the implementation of formal integration policies, by addressing two pivotal questions: (1) What are the spatial and temporal characteristics of LUCC in the GBA during the pre-integration period from 1990 to 2018? (2) What are the driving factors behind LUCC in the GBA during this period, and how did they influence these changes?

To answer these questions, this study concentrates on the expansion of a BUA, a primary and most conspicuous form of LUCC in the GBA. This study initially applies Moran's Index, based on multiple big data sources, to explore the spatial–temporal distribution characteristics of LUCC in the GBA before the implementation of formal integration policies. Subsequently, the Geographically Weighted Regression (GWR) model is used to identify key factors driving BUA expansion and their influence in terms of extent and direction, which varies across different areas in the GBA. This study provides a rare empirical perspective on the formation of megacity regions' spatial structures, which are shaped by LUCC in the absence of state-led formal integration frameworks. It offers valuable insights not only for understanding megacity regions globally but also imparts critical experience from China's Greater Bay Area for managing cross-border and cross-administrative urban expansion worldwide.

2. Literature Review

2.1. Megacity Regions: Formal and Informal Pathways of Formation

Megacity regions have developed through two distinct pathways: formally planned integration (top-down) and informal bottom-up processes. Both pathways exhibit dis-tinct advantages and limitations in the structuring of spatial forms and governance mechanisms. Bottom-up processes foster greater adaptability and encourage local initiatives, but they can also lead to fragmentation in governance and result in uncoordinated spatial development. Conversely, top-down models demonstrate strengths in coordinated planning and infrastructure provision, but they may also show limited flexibility and responsiveness to local conditions. Table 1 summarises and compares the different formation pathways of megacity regions across various geographical and institutional contexts [1,2,14–18].

Table 1. Pathways of megacity regions' formation.

Region	Type of Formation	Integration Policy	LUCC Led by	Key References
Northeast Corridor (US)	Bottom-up (informal)	No integrated planning	Private sector and commuters	[14,15]
San Francisco Bay Area (US)	Bottom-up (informal)	Weak/formal designation	Market forces, suburbanisation	[16]
Tokyo Bay Area (Japan)	Top-down (formal)	National urban plans	State-led land regulation	[17]
GBA before 2019 (China)	Hybrid (Informal to Formal)	Lacked unified plan pre-2019	Local governments and industrial developers	[1,2,18]

In many western contexts, megacity regions are the result of spontaneous suburbanisation, economic complementarities, and commuting flows, which develop functional linkages without unified policy frameworks [15]. This phenomenon was first observed

by Gottmann [14] in the Northeastern United States, where he introduced the concept of "megalopolis" to describe the emerging urban continuity. Building upon this, Harrison and Hoyler [16] subsequently identified the San Francisco Bay Area as a typical example of a bottom-up case and introduced the concept of the megaregion, which is primarily shaped by local land development and suburban expansion. The spatial integration of these areas is consistently reflected in a significant expansion of the BUA. Therefore, LUCC serves as an important spatial indicator for observing emerging changes in regional spatial structure. Despite the increasing functional and land integration ties, these bottom-up megaregions frequently operate under fragmented governance structures and lack spatial coordination at the institutional level [16]. In contrast, East Asian megacity regions, such as those in Japan, have mainly adhered to top-down, state-led models of spatial integration. Such strategic interventions are often realised through targeted land development practices—the Tokyo Bay Area, for example, was shaped through national spatial strategies that included industrial relocation, infrastructure expansion, and land-use controls [17]. These interventions resulted in highly coordinated regional land-use structures under strong central oversight.

Building on this debate, we follow Harrison and Gu [3] in using the notion of informal regionalism to capture bottom-up and decentralised forms of megaregional integration. Informal regionalism refers to processes through which regional integration is advanced primarily by dispersed state actors (such as municipal governments), market forces, and cross-border infrastructure, before a formal, unified institutional framework is established. In the GBA, informal regionalism has been expressed through the early formation of cross-border production and service chains between Hong Kong/Macao and mainland cities (for example, export-processing industries, tourism, and finance), as well as through entrepreneurial local governments in the Pearl River Delta using land development and infrastructure projects under the "one country, two systems" framework to promote cross-boundary functional integration. In this paper, we operationalise informal regionalism empirically by reading LUCC patterns—particularly the emergence of cross-boundary BUA clusters revealed by global and local Moran's I—as the material imprint of these processes, and by using the spatial heterogeneity of GWR coefficients to locate where and how different districts, through distinct combinations of socio-economic and natural drivers, have contributed to bottom-up megaregional integration.

China presents a more multi-layered picture of state intervention, where the boundaries between formal and informal regionalisation become ambiguous. On one level, successful stories of megacity regions, such as the Yangtze River Delta and the Jing-Jin-Ji region, have been explicitly promoted through central government policies, with clear administrative, fiscal, and infrastructural frameworks [1,2]. However, many of China's spatial transformations have stemmed from local government initiatives, where local authorities act as spatial entrepreneurs, employing land development, cross-boundary infrastructure, and policy instruments to promote functional regionalisation in the absence of central coordination [19]. Hence, it becomes challenging to determine whether such megaregional development mainly stems from a top-down strategic vision or from bottom-up local responses that were subsequently recognised and institutionalised by the central state [3]. This complexity contrasts with the prevailing perspective in Western academic literature, which frequently characterises China's spatial planning-led LUCC as a highly centralised and hierarchical process driven predominantly by state-led initiatives [17].

The GBA exemplifies a typical case of hybrid megaregional development, initially propelled by entrepreneurial local governments and market mechanisms, and only later brought under a formal state-led integration framework after 2018. Before China's land reform in the early 1990s, urban land in mainland cities was exclusively state-owned, providing limited autonomy for local spatial initiatives [20]. With the implementation of

China's reform and opening-up policy, local governments also gained greater autonomy, and the land market became more liberalised, facilitating processes mainly driven by local governments and market forces. Following the return of Hong Kong and Macao and the implementation of the "one country, two systems" framework, cities in the Pearl River Delta actively pursued industrial relocation, port development, and cross-boundary infrastructure projects. These locally coordinated efforts significantly reshaped regional land-use patterns, despite the absence of formal national integration policies during this period [21]. The formal introduction of the Outline Development Plan for the GBA in 2019 established a unified integration framework, marking a new stage of centrally coordinated spatial integration and regional land-use planning. Therefore, examining how the GBA has developed its fundamental spatial structure through bottom-up pathways in the absence of a state-led integration framework contributes to a deeper understanding of the evolutionary mechanisms of megacity regions and offers important insights for future spatial governance and planning at the national level.

2.2. Previous Studies

2.2.1. Land Use and Cover Change

LUCC studies how natural processes and human activities alter the Earth's surface, which has important implications for environmental management, urban planning, policy-making, and sustainability [9,22]. Consequently, two fundamental research questions pertaining to land-use change have been identified through the support of the joint IGBP–IHDP within the LUCC project. These questions are the characteristics and drivers of LUCC. Geist and McConnell [23] put forward that conversion and modification are the two forms of LUCC. Conversion is a change from one land-use or cover category to another, such as cropland to a built-up area. Additionally, modification refers to changes within the same land-use or cover category (e.g., cover change in forest land). Human activities lead to LUCC, thereby increasing the diversity of land use and cover types. Consequently, a single land-cover category may fulfil multiple functions. For example, agricultural land can consist of both cultivation areas and residential zones. Conversely, a singular land-use system may encompass diverse land types, such as an urban setting integrating agricultural zones, BUA, and forested regions within a city.

BUA expansion refers to the process by which natural or rural land is converted into impervious surfaces, such as roads, buildings, and infrastructure, primarily driven by urbanisation and population growth. It is widely recognised as one of the most dominant and observable forms of LUCC, particularly in megacity regions, where rapid urban development is prevalent [24,25]. Therefore, analysing the spatial and temporal dynamics of BUA expansion provides critical insights into urban growth spatial patterns, land development intensity, and environmental pressures [22]. LUCC studies urban and regional units, as well as BUA, at different spatial levels. At the global level, Zhou and Zhong [26] delineated the spatial extent and conceptual dimensions of a BUA across a range of internationally representative megacities. They reviewed the spatial and temporal characteristics of the scale and structure of a BUA in international metropolises. At the country level, Ran [27] studied the characteristics of BUA expansion among large and medium-sized cities in China during the 1990s. They found that the most rapid expansion of a BUA in China occurred in the eastern region, while the slowest expansion was in the central region, with a significant decline in urban land per capita in the latter. At the regional level, Fang and Yu [11] examined three significant BUA zones in China and identified the characteristics of a BUA in large cities in China. While these studies provide valuable insights, the majority focus on aggregate urban units or city-level trends. However, little attention has been paid to how the expansion of a BUA reflects deeper regional integration logics in megac-

ity regions, especially those experiencing institutional change or lacking formal spatial coordination mechanisms.

2.2.2. Drivers of Built-Up Area Expansion

Numerous studies estimate the driving factors of LUCC. In terms of the driving factors of LUCC, Geist and McConnell [23] examined LUCC outcomes stemming from the interaction between environmental and social dimensions across various temporal and spatial contexts. The study finds that LUCC can be affected by nature and socio-economic factors. The effects of natural factors on the spatial patterns of land use/cover tend to persist over extended periods. However, in the short term, natural characteristics such as geology, hydrology, and soil properties evolve slowly and exert a relatively limited influence on land-use/cover dynamics. In contrast, socio-economic factors result from human activities related to LUCC and development processes, which directly alter these patterns. For instance, population growth has a direct human impact that increases demand for land resources. In addition, socio-economic drivers include political frameworks, economic conditions, technological advantages, and industrial structures [22].

Among the various manifestations of LUCC, the expansion of a BUA in urban settings is arguably the most notable. This type of land transformation is also influenced by natural and socio-economic factors, whereas empirical studies typically highlight the latter because of their higher variability and more significant short-term effects. Lloyd [28] finds that the urban population and gross domestic product (GDP) are positively correlated with the expansion of a BUA in 145 cities in China over the past 15 years. Wu and Li [19] argue that urban planning is the most central driver of BUA expansion. The impact of economic development on BUA expansion is a more substantial effect than the impact of demographic change. From most of these studies, natural and socio-economic factors are the primary drivers of the expansion of a BUA. However, Chen and Chang [29] argue that natural and socio-economic factors impact the expansion of a BUA. Therefore, Chen and Chang [29] selected demographic variation, economic growth, real-estate investment, and industrial structure as socio-economic factors, while the area of water and density of transport road networks could serve as indicators of natural factors. In rapidly urbanising megacity regions, road and water networks often facilitate leapfrog development, enabling construction to bypass ecological buffers and accelerating the conversion of peripheral agricultural and forest land. Under global environmental change, this pattern heightens exposure to climate hazards and accelerates biodiversity loss, thereby underscoring the need for active protection measures such as ecological redlines, floodplain zoning, and habitat-connectivity planning.

Although these insights are valuable, most current studies are limited to urban or metropolitan areas, restricting our understanding of the main factors influencing the spatial development and evolution of megacity regions. As BUA expansion continues, metropolitan zones emerge around core cities, and the physical boundaries between neighbouring urban areas begin to dissolve, gradually restructuring formerly independent cities into functionally interdependent urban clusters. However, in many cases, administrative and institutional arrangements remain fragmented, and formal policy integration often lags behind actual patterns of urban growth. Following China's 1990 urban land reform, these dynamics became particularly pronounced in the GBA, which occupies only about 0.6% of China's land area but contributed 12.57% of national GDP in 2018; such high-intensity land development has been accompanied by the loss of coastal wetlands and increasing fragmentation of agricultural and forest land. These trade-offs call for an ecosystem philosophy of spatial development, in which ecosystems and their services are treated as fundamental units of spatial planning and land allocation so that economic growth is pursued while

maintaining ecological integrity. In such contexts of fragmented governance, examining the drivers of BUA expansion offers critical insights into how regional spatial structures emerge prior to formal integration. This study adopts the LUCC analysis method to quantitatively examine the spatial structure of megacity regions in the GBA from 1990 to 2018—a period spanning from China's 1990 urban land reform, which introduced land-transfer policies, to the GBA's formal recognition as a megacity region.

3. Data and Methods

3.1. Study Area

Figure 1 illustrates the study area, the Guangdong–Hong Kong–Macau Greater Bay Area (GBA), located in southern coastal China (21°32′–24°26′ N, 111°20′–115°24′ E). The GBA comprises 11 cities: Hong Kong, Macau, Guangzhou, Shenzhen, Zhuhai, Foshan, Huizhou, Dongguan, Zhongshan, Jiangmen, and Zhaoqing.

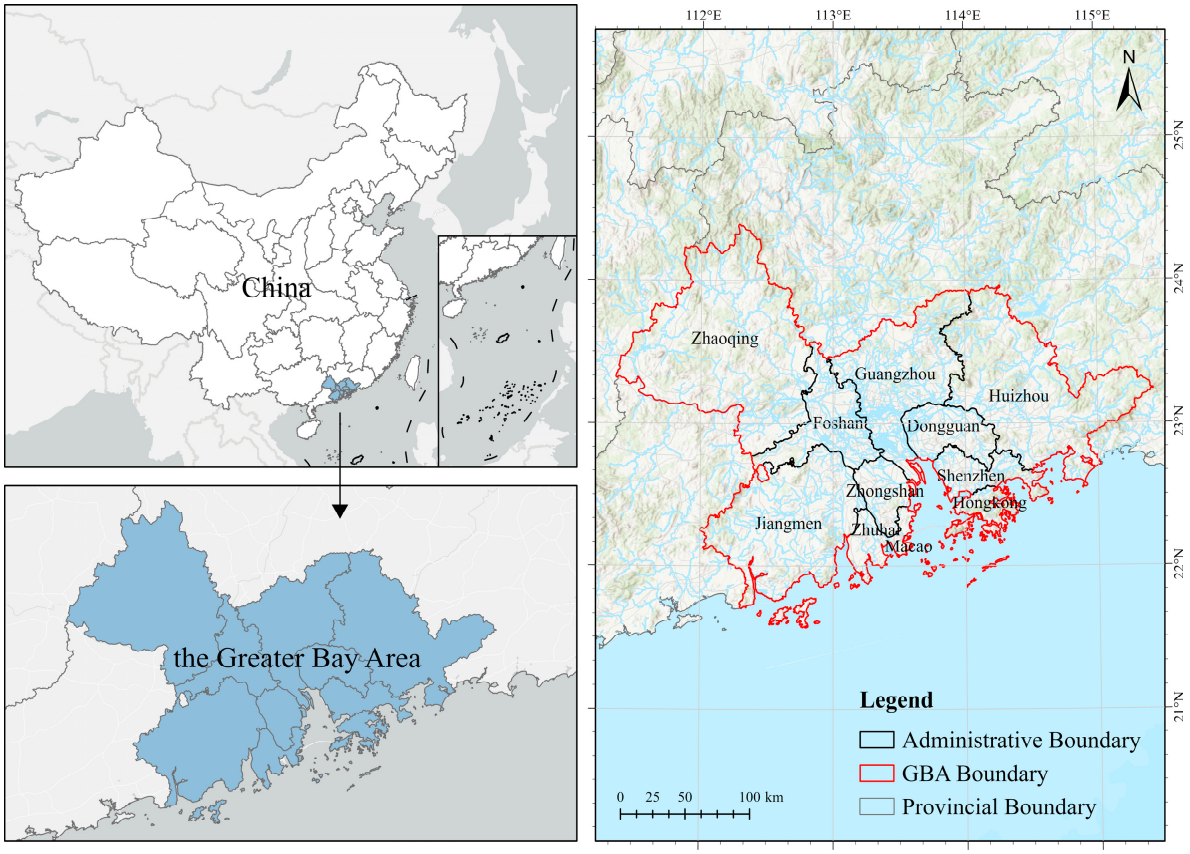

Figure 1. Eleven cities in the Guangdong–Hong Kong–Macau Greater Bay Area (by author).

According to China's Bureau of Statistics, the region's total area was estimated at 56,000 km^2, and about 110 million people were in this region in 2018 (Table 2). It is one of China's most economically advanced and globally integrated regions, showcasing rapid urbanisation. The area hosts diverse industries, including high-tech sectors, manufacturing, international enterprises, financial services, and renowned educational institutions. While occupying only 0.6% of China's land area, the GBA contributed 12.57% of the nation's GDP in 2018, amounting to RMB 10.32 trillion (USD 1.64 trillion).

Table 2. GBA eleven cities' GDP and population data from 1998 to 2018. (Source: National Bureau of Statistics of China, Guangdong Statistical Yearbook, Hong Kong and Macao Statistical Yearbooks).

City/Year	1990		2000		2010		2018	
	Pop	GDP	Pop	GDP	Pop	GDP	Pop	GDP
GBA	2395.21	2842.5	3030.79	13,446.49	3492.87	30,226.51	6797.7	100,326.9
Guangzhou	555.41	139.55	646.71	1260.31	750.53	187.85	1449.84	21,503.15
Shenzhen	51.50	41.65	99.16	842.79	181.93	5035.77	1190.84	22,490.06
Foshan	258.64	56.57	311.06	563.72	354.48	2383.18	765.67	9398.52
Huizhou	18.21	16.63	255.90	229.57	297.58	805.11	475.55	3830.58
Jiangmen	334.61	47.17	371.81	362.73	386.24	801.70	456.17	2690.25
Zhongshan	107.35	23.23	125.25	175.82	140.82	885.72	326.00	3430.31
Dongguan	123.01	30.02	143.65	296.45	165.65	2188.19	749.66	7582.09
Zhaoqing	309.11	22.22	355.97	163.66	396.48	435.95	408.46	2110.01
Zhuhai	42.59	11.11	63.24	182.69	89.60	640.53	176.54	2675.18
Hong Kong	552.46	2350	615.60	8931.25	681.30	11,106.25	733.66	21,456.75
Macau	42.32	104.30	42.44	437.5	48.26	756.25	65.31	3160.00

Note: All statistics data were obtained from local statistics yearbook. Pop unit: ten thousand; GDP unit: RMB 100 million; RMB 1 is about USD 0.16.

3.2. Data

The database collection used in this study consists of remote-sensing and statistical data. Remote-sensing data include a remote-sensing study area, river and road data, and land-use data. The statistical data contain socio-economic and natural data of the study area. The remote=sensing data are from China Land Remote Sensing Monitoring Datasets (CLRSMD) published by the China GIS Centre in 2020. The LUCC data acquisition is based on Landsat TM digital imagery in CLRSMD and employs a digital human–computer interactive remote-sensing fast-extraction method. Gong and Li [30] rigorously validated the database, demonstrating overall classification accuracies exceeding 90%. Specifically, the remote-sensing datasets of LUCC comprise annual TM imagery with a spatial resolution of 30 m × 30 m, covering four time points: 1990, 2000, 2010, and 2018 (Appendix A).

Based on China's land classification policy, the remote-sensing data were processed and reclassified into six primary land-use types—agricultural land, forest land, grass land, water, built-up area, and unused land—using ArcGIS 10.0 (Figure 2). The annual database can provide timelier and more detailed LUCC information on the GBA (Table 3). LUCC remote-sensing data show land-use data at the district and county level, including 11 cities and 52 districts in the GBA.

Table 3. Land-use/cover data of the study area in 1990, 2000, 2010, and 2018 (Source: China Land Remote Sensing Monitoring Datasets).

Land-Use Classification	1990		2000		2010		2018	
	Area/km^2	%	Area/km^2	%	Area/km^2	%	Area/km^2	%
Grass	1272.3	2.3	1222.5	2.2	1099.6	2.0	1240.7	2.2
Agriculture	15,919.9	28.9	14,443.1	26.2	12,641.3	22.9	12,408.5	22.4
Forest	30,910.6	56.0	30,629.0	55.5	30,044.0	54.3	29,677.1	53.7
Construction	3132.5	5.7	4456.3	8.1	7371.1	13.3	8195.8	14.8
Water	3852.5	7.0	4369.9	7.9	4091.4	7.4	3770.5	6.8
Unused land	74.2	0.1	41.0	0.1	45.1	0.1	8.1	0.0

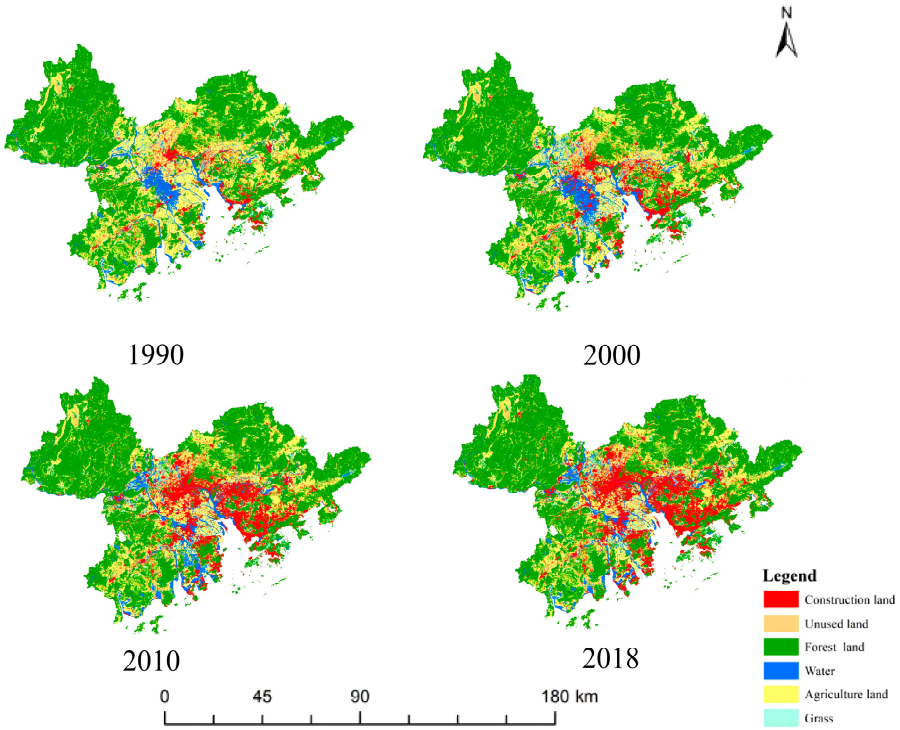

Figure 2. GBA LUCC remote-sensing dataset of GBA in 1990, 2000, 2010, 2018.

The variable's statistical data details are reported in Appendix B, including population, financial income, GDP, total real-estate investment, industry structure, and road and water area density. The statistics are drawn from China Statistical Yearbooks [31], China City Statistical Yearbooks [32], Guangdong Statistical Yearbooks [33], and Hong Kong and Macau Statistical Yearbooks [34,35]. The China Statistical Yearbook is a comprehensive annual publication representing the economic and social development of the People's Republic of China, published annually by the National Bureau of Statistics of China. The China Statistical Yearbook (2019) systematically records statistics on all aspects of China's economy and society over the period from 1990 to 2018, and most scholars use the Statistical Yearbook for China's society and economy research [31].

4. Methods

4.1. Moran's Index Model

This study employs spatial autocorrelation analysis to investigate the spatial dependence and heterogeneity of land-use patterns in the GBA. Specifically, global Moran's I indices are calculated for three major land-use types—BUA, forest land, and agricultural land—across multiple periods to assess changes in overall spatial autocorrelation and regional imbalance. In addition, local Moran's I analysis is conducted for the BUA to identify localised clusters that reflect uneven patterns of BUA scale within the megaregion. In the selection of spatial units, city-level administrative units are widely used as spatial units in megacity region research to capture inter-city spatial variation [15]. Thus, the spatial units used in the Moran's I analysis are the 11 administrative cities within the GBA. To ensure comparability across administrative units of varying sizes, the spatial variables for all three land-use types are standardised by dividing the land-use area by the total land area of each city [36]. As each city in the GBA shares a common boundary with at least one other city, a first-order Queen contiguity spatial weights matrix is constructed to define inter-city spatial relationships. The matrix is row-standardised to ensure consistent spatial influence across all units [36,37].

The Moran's index model, introduced by Pap [38], is widely used for global and local spatial autocorrelation analyses. Spatial autocorrelation measures can be classified into two categories: global and local. The global Moran's I indicates whether spatial clustering exists across a region, but does not specify the locations of these clusters. In contrast, the local Moran's I identifies where clustering occurs. Specifically, a Moran's I value greater than 0 reflects a positive spatial correlation, with higher values indicating stronger correlations. In contrast, a value less than 0 indicates a negative spatial correlation, signifying a greater spatial variation. A Moran's I of 0 represents spatial randomness. This index has been extensively applied in land-use and cover research to explore spatial clustering characteristics [39].

4.1.1. Global Moran's Index

The global Moran's I measures spatial autocorrelation across an entire study area, effectively capturing the spatial relationships of attribute values throughout the region [40]. It assesses whether the spatial distribution of a variable is correlated with neighbouring values [41]. This measure is widely used in spatial statistical analyses, and the formula is presented as follows:

$$I = \frac{n\sum_{i=1}^{n}\sum_{j=1}^{n}\omega_{ij}(x_i-\overline{x})(x_j-\overline{x})}{\sum_{i=1}^{n}\sum_{j=1}^{n}\omega_{ij}\sum_{i=1}^{n}(x_i-\overline{x})^2} = \frac{\sum_{i=1}^{n}\sum_{j\neq i}^{n}\omega_{ij}(x_i-\overline{x})(x_j-\overline{x})}{S^2\sum_{i=1}^{n}\sum_{j\neq i}^{n}\omega_{ij}} \quad (1)$$

In this formulation, the spatial weight between features i and j is represented by ω_{ij}. The attribute values corresponding to locations i and j are denoted as x_i and x_j, respectively. The mean attribute value is expressed as $\overline{x}$, while n indicates the total count of features within the dataset.

4.1.2. Local Moran's Index

The local Moran's I, developed as a Local Indicator of Spatial Association (LISA) by Anselin [37], serves to measure spatial autocorrelation at a localised scale. This index quantifies the extent of spatial clustering within individual regions by identifying significant agglomeration patterns among neighbouring regions within similar values. The sum of all local Moran's I values is proportional to the global Moran's I for the entire dataset. LISA maps categorise spatial clusters into four types: High–High (HH), Low–Low (LL), High–Low (HL), and Low–High (LH).

Local Moran's I is formulated as follows, where each parameter has the same meaning as in Equation (1):

$$I_i = \frac{(x_i-\overline{x})}{S^2}\sum_{j=1}^{n}\omega_{ij}(x_j-\overline{x}) \quad (2)$$

4.2. Geographically Weighted Regression Model

Geographically Weighted Regression (GWR), as proposed by Fotheringham and Brunsdon [42], represents a localised adaptation of ordinary least squares (OLSs) regression. In contrast to traditional regression models, GWR effectively addresses spatial heterogeneity by generating local regression results for each observation. This methodology enables the identification of spatially varying relationships between dependent and independent variables. The outputs produced by GWR include local parameter estimates and corresponding t-test values, thereby offering a comprehensive visualisation of spatial non-stationarity. With the framework of LUCC analysis, GWR facilitates the understanding of how various driving factors influence BUA expansion across different geographical locations.

The formula of the GWR model is shown below:

$$Y_j = \beta_0(u_j, v_j) + \sum_{i=1}^{p} \beta_i(u_j, v_j) X_{ij} + \varepsilon_j \quad (3)$$

In this formula, Y_j represents the dependent variable for observation j, and X_j denotes the independent variable X at the location of observation j. The coordinates u and v specify the spatial position of observation j. The term $\beta_0(u_j, v_j)$ refers to the intercept at the given location, while $\beta_i(u_j, v_j)$ signifies the localised regression coefficient for the independent variable X at observation j [43].

In this research, the expansion scale of built-up area (ESBUA) is identified as the dependent variable (Y), based on prior studies (Table 1). This variable serves as a proxy for urban LUCC, given that the rapid expansion of the built-up area has a significant impact on the urban LUCC. According to the literature reviews, socio-economic and natural factors are recognised as two primary driving forces in this study [44,45]. The population size, average gross domestic product (AGDP), total real estate investment, percentage of tertiary industry structure, and local financial income can be selected as proxies for socio-economic factors within the GWR model [39]. In the context of natural driving forces, two mainly independent variables are identified: the density of the road network (D_ROAD) and a variable for the water area (A_WATER). While the road network density (D_ROAD) is typically associated with human infrastructure, it is considered a natural driving force in this study due to its direct impact on physical landscapes at the megacity regional scale. In addition, D_ROAD serves as a form of external connectivity that acts as an initial condition or natural endowment for the development of new towns and cities [46,47]. The water area (A_WATER), which encompasses lakes, seas, and rivers, is identified as a natural driver because it represents a fundamental geographic constraint and an ecological determinant. It significantly influences land use by shaping urban boundaries, flood risks, and hydrological processes [48,49]. For data processing purposes, the monetary values of AGDP and finance income are converted to RMB based on the exchange rate from 2018. The "Distance Analysis" and "Zonal Statistics" tools in ArcGIS are employed to calculate A_Water and the D_ROAD data. Both variables are expressed in kilometres.

The variable details of the GWR model are shown in Table 4. In the selection of spatial units, to further analyse the driving factors of built-up area (BUA) expansion and their spatial heterogeneity, all variables were measured at the district (county) scale within the GBA and subsequently analysed using the GWR model. The GWR model can be used to eliminate the influence of city size and measure the extent of BUA expansion in different cities during the same period. In addition, this allowed for quantifying the impacts of socio-economic and environmental factors on BUA expansion, as well as examining the spatial heterogeneity of these relationships across the GBA [50]. To avoid the influence of differing units of measurement, all variables were standardised prior to analysis. Prior to GWR estimation, multicollinearity among explanatory variables was tested using the Variance Inflation Factor (VIF). An adaptive bandwidth was selected based on the minimisation of the corrected Akaike Information Criterion (AICc), and a bi-square kernel function was employed to determine spatial weights [42]. To assess the performance of GWR, model results were compared with those of a global ordinary least squares (OLSs) regression.

Table 4. Description of Variables.

Variable Types	Variable	Variable Code	Description	Expectation	Data Sources
Expansion of built-up area	Y	ESBUA	Expansion scale of the built-up area (ESBUA) from 1990 to 2018 (Km^2) = [(BUA in 2018 − BUA in 1990)] (Km^2)	/	Gong, Li [30]
Socio-economic factors	X1	AGDP	Average Gross Domestic Product growth from 1990 to 2018 (RMB 100 million)	+	China Statistical Yearbooks [31], China City Statistical Yearbooks [32], Guangdong Statistical Yearbooks [33], and Hong Kong and Macau Statistical Yearbooks [34,35].
	X2	POP	Population growth from 1990 to 2018 (%) (10,000 people)	+	
	X3	RE	Total real-estate investment from 1990 to 2018 (RMB 100 million)	+	
	X4	INCOME	Local financial income in 2018 (RMB 100)	+	
	X5	I3	Percentage of the third industry structure in 2018 (%)	+	
Natural factors	X6	D_ROAD	Density of the road in 2018 (Km/Km^2)	−	
	X7	A_Water	Water area in 2018 (Km^2)	+	

Note: Y: proxy of increasing built-up area; X1, X2, X3, X4, X5: proxy of socio-economic driving factors; X6, X7: proxy of natural driving factors. "+" indicates an expected positive relationship; "−" indicates an expected negative relationship; "/" indicates not applicable (no expectation specified).

5. Empirical Results

5.1. Spatial Characteristics of LUCC in the GBA

5.1.1. Built-Up Area Expansion in the GBA

Since urban expansion is the most direct and measurable manifestation of LUCC in megaregion contexts, BUA expansion is adopted as the primary indicator of LUCC in this study. The GBA region has undergone significant changes in urban BUA over the last three decades (Figure 3). From 1990 to 2018, the area designated for urban development increased by approximately 13-fold, as shown in Section 3.1. Guangzhou, Shenzhen, Foshan, and Dongguan have experienced the most significant changes, with an average range of 1256.49 km^2. Conversely, Hong Kong and Macau have witnessed relatively minor alterations in their urban landscapes, with increases of 118.53 and 6.98 km^2, respectively.

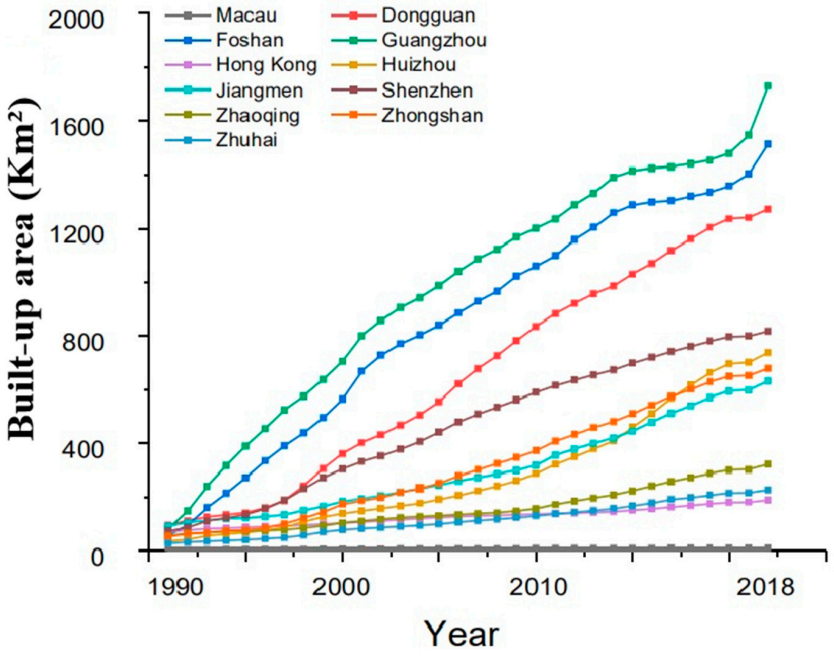

Figure 3. The temporal changes of the built-up area of 11 cities in the GBA during 1990–2018.

Figure 4 indicates the detailed spatial and temporal changes in the BUA within the GBA from 1990 to 2018. The varying colours represent the expansion of the BUA across different years, while the blank space denotes other types of land use, such as agricultural land and forest land. From a spatial distribution perspective, the patterns of BUA expansion in the GBA at various stages exhibit several important characteristics.

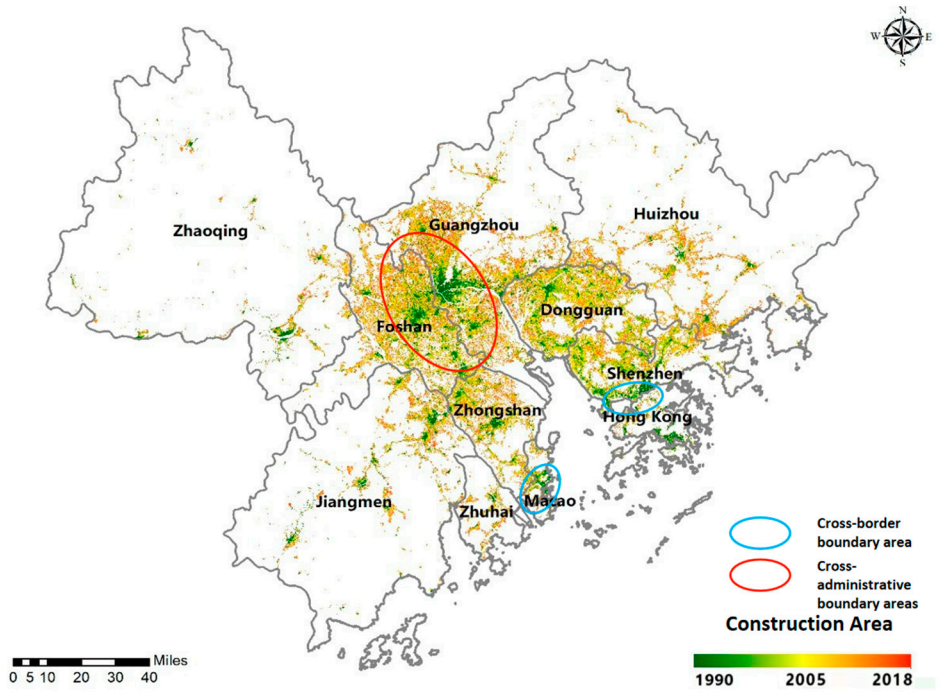

Figure 4. GBA built-up area expansion.

1. Between 1990 and 2018, the BUA in the GBA experienced significant expansion. This transformation led to an extension of urban-centre boundaries, while simultaneously reducing the areas designated for forest and agricultural land. Notably, Foshan, Dongguan, Zhongshan, and Shenzhen have exhibited the most significant BUA expansion.
2. In 1990, the original BUA was mainly concentrated in Hong Kong, Macau, the central area of Foshan, the central area of Dongguan, and the western part of Guangzhou. By 2018, BUA in the GBA had shifted to mainly concentrated in the central area adjacent to the Pearl River Estuary. Notably, Zhaoqing, Jiangmen, Huizhou, and Zhuhai continued to possess undeveloped land by 2018.
3. During 1990–2018, the informal integration period, infill development at the Guangzhou–Foshan boundary led to the emergence of a cross-administrative urban core.
4. In contrast, Zhuhai, Hong Kong, and Macao, which are multi-island cities, exhibit BUA expansions that mainly occur in clusters, thus establishing a polycentric spatial distribution pattern.
5. Shenzhen and Zhuhai are among the first cities to be developed in proximity to Hong Kong and Macao, illustrating the significant influence of these regions on the LUCC trajectory. During 1990–2018, LUCC in the Shenzhen–Hong Kong and Zhuhai–Macao corridors gave rise to two prominent cross-border fundamental core structures.

5.1.2. Global Spatial Attributes of LUCC in the GBA

This study employs Moran's I index to examine spatial and temporal relationships in GBA land-use/cover data. The calculation of this index incorporates land-use/cover datasets and statistical measures for different land categories across the 11 regional divisions of the GBA from 1990 to 2018. The findings highlight the degree of spatial connections

between land types and reveal the structural clustering characteristics within the GBA region, as shown in Figure 5.

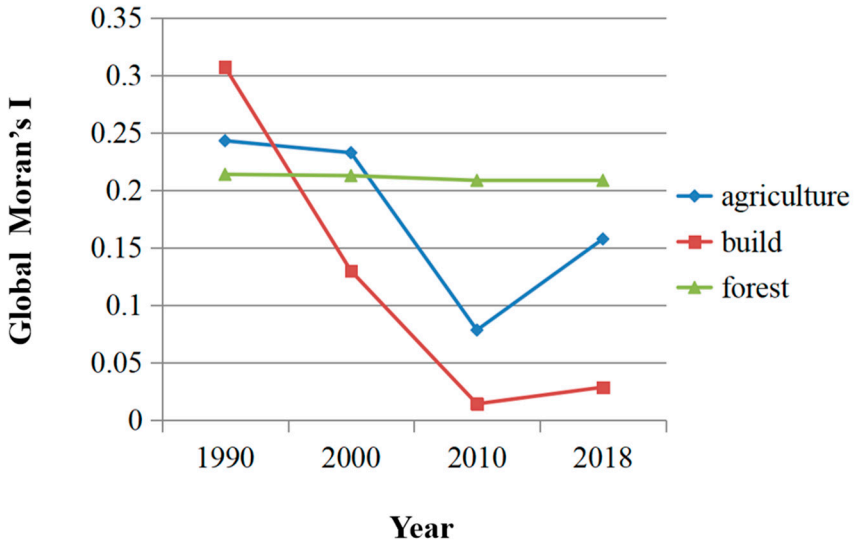

Figure 5. Global Moran's I of land use/cover of the GBA from 1990 to 2018.

From 1990 to 2018, Figure 5 indicates that the value of Moran's I index ranges from 0.078 to 0.32, depending on land use/cover. This reflects the varying socio-economic and environmental situations. Consequently, Moran's I index values for land use/cover refer to distinct traits and patterns associated with these categories. In terms of the land use/cover of the research area, spatial autocorrelation is evident for Forest Land (FL), Agricultural Land (AL), and BUA. Overall, while Moran's I index for forest land exhibits a declining trend over time, AL and BUA experienced a turning point around 2010.

From 1990 to 2010, Moran's I index for AL showed a continuous decline, dropping from approximately 0.25 to 0.08. This trend corresponds with a sharp decrease in agricultural land proportion, which declined from 28.9% in 1990 to 22.9% in 2010. The spatial fragmentation of AL increased during this period as large tracts of farmland were increasingly converted into other land types, particularly construction land. This fragmentation contributed to a weakening spatial clustering pattern and thus a lower Moran's I. Interestingly, after 2010, the Moran's I index for AL rebounded, increasing to around 0.16 by 2018. This occurred despite a continued decline in the proportion of agricultural land, which further decreased to 22.4%. The observed rebound in spatial autocorrelation suggests that the remaining agricultural parcels became more spatially concentrated—possibly due to targeted preservation of core agricultural zones or consolidation of land use. Consistent with prior studies, these patterns align with documented land-cover trajectories in the GBA, including the stabilisation or consolidation of cultivated land under prime farmland protection, incremental woodland gain from ecological restoration, and constrained conversion of agricultural parcels at the urban fringe [26]. For forest land (FL), Moran's I index remained relatively stable throughout the study period, hovering slightly above 0.2. This consistency is reflected in the relatively stable land proportion as well: FL accounted for 56.0% in 1990, 55.5% in 2000, 54.3% in 2010, and 53.7% in 2018. Although minor changes occurred, they were spatially uniform, resulting in a steady spatial clustering pattern.

In contrast, the BUA has experienced substantial growth, increasing from 5.7% of the study area in 1990 to 14.8% by 2018. The fragmented spatial distribution of agricultural and forested lands has reduced aggregation due to the conversion of a substantial portion of these areas into a BUA, which holds higher economic value. The positive Moran's I index for the BUA from 1990 to 2018 indicates that a BUA within the GBA exhibits a

pattern of positive spatial autocorrelation. This outcome is associated with the rapid urban expansion associated with the construction activities across various cities and regions. Between 1990 and 2010, however, the spatial correlation of land use and cover in the GBA progressively declined as influenced by the surrounding urban growth. Following this period, after 2010, Moran's I index for the BUA began to rise again, signalling an increase in BUA coverage within the GBA. This trend highlights the spatial duality that emerged between 2010 and 2018. These findings align with the evolution of China's real-estate sector from 2008 to 2018, characterised by significant industry expansion.

5.1.3. Local Spatial Attributes of LUCC in GBA

LISA metrics are calculated for the BUA in 1990, 2000, 2010, and 2018. The corresponding LISA distributions are visualised using a z-test with a 95% confidence level (Figure 6). Local spatial relationships among variables within and adjacent to the region can be classified into four types based on the LISA distribution map: high–high, high–low, low–high, and low–low spatial clusters. The high–high category indicates that the area and its neighbouring regions exhibit elevated attribute values. Conversely, the high–low type suggests that the area has lower attribute values compared to its surroundings. In contrast, the low–high and low–low types reflect opposite trends. The high–high and low–low indices identify patterns of clustering and similarity, highlighting a strong positive spatial connection among regions. Meanwhile, a significant negative spatial relationship and significant heterogeneity emerge across low- to high-range regions.

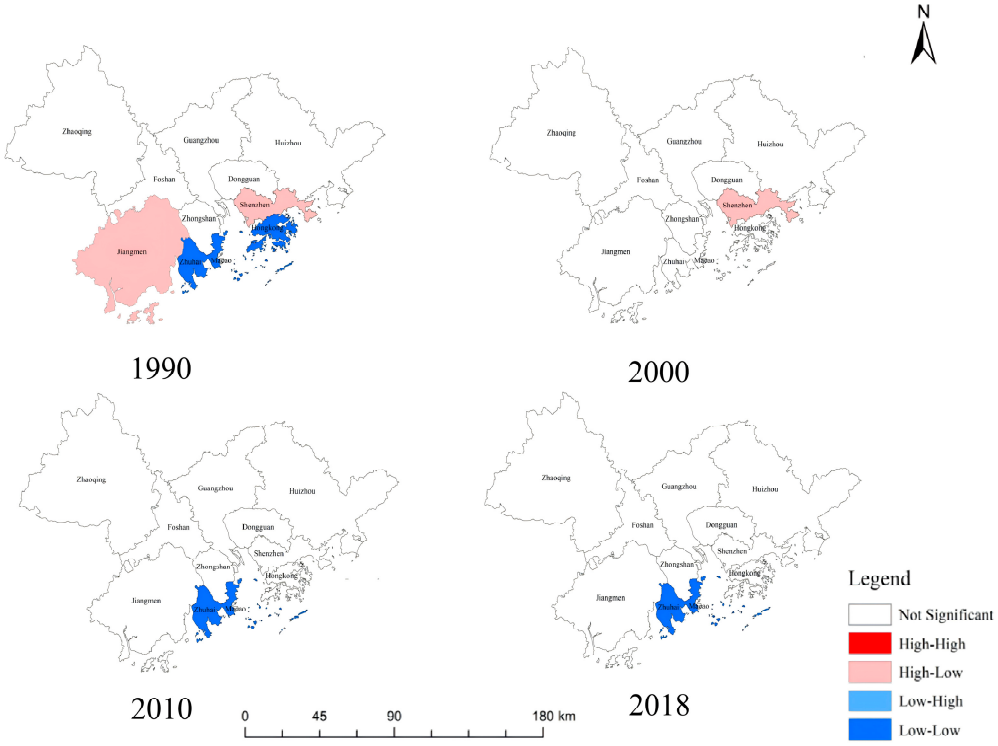

Figure 6. LISA cluster map of the built-up area of the GBA in 1990, 2000, 2010, 2018.

The LISA cluster results clearly illustrate that within the Greater Bay Area, significant high–low spatial clusters were primarily concentrated in Shenzhen and Jiangmen before 2000; however, these high–low spatial correlation patterns gradually disappeared in subsequent periods. Shenzhen's development began relatively early, with its BUA reaching 349.2 km^2 by 1990. Between 1990 and 2000, a strong high–low spatial correlation was observed between Shenzhen's BUA and its neighbouring areas, with a significance level of 99%. In the same period, Jiangmen experienced the third-largest expansion in the BUA

among the 11 cities in the study area, surpassing 1000 km^2. This increase was significantly higher than in adjacent areas, resulting in a notably high–low spatial relationship with a significance level of 99%.

In terms of BUA growth, Shenzhen ranked third between 1990 and 2000 and first from 2000 to 2005, outperforming other cities in the region. This remarkable growth can be attributed to China's reform and opening-up policies, which propelled Shenzhen to become a leading city in the GBA by 2010. Although Shenzhen currently ranks third in the region, other cities, such as Dongguan, have witnessed steady economic development since 2010. This period saw substantial increases in BUA, but the previously observed high–low spatial correlation patterns gradually disappeared.

Within the GBA, significantly low–low spatial clusters were primarily concentrated in Zhuhai, Macao, and Hong Kong before 2000. After 2000, the low–low spatial correlation involving Hong Kong gradually disappeared, leaving Zhuhai and Macao as persistent low–low cluster areas. This pattern indicates that these cities and their adjacent areas consistently exhibited a low scale of BUA, reflecting either inherently small urban sizes or limited development during the early formation phase. Hong Kong's transition away from the low–low clustering pattern after 2000 suggests significant BUA growth in Hong Kong and increased integration with surrounding areas. In contrast, the persistent low–low clusters in Zhuhai and Macao highlight ongoing constraints or a slower pace of urban expansion. Macao's enduring low–low clustering could be attributed to its inherently small urban scale, while the limited BUA expansion in Zhuhai and its surrounding cities underscores persistent regional spatial imbalances. These LISA results reveal the spatial imbalance of built-up development within the GBA and reflect differentiated stages of regional urbanisation.

5.2. Driving Factors of Built-Up Area Expansion

This study uses the GWR model to explore the driving factors of BUA expansion in the GBA. The findings are compared with those obtained from traditional OLSs model results. To ensure appropriate variable selections, the Variance Inflation Factor (VIF) analysis is conducted to test for multicollinearity among variables. As presented in Table 5, all VIF values for the statistical variable are below 7.5, indicating an absence of multicollinearity across all variables. The VIF test standards are discussed in Section 3.2. Consequently, each variable listed in Table 5 is subjected to regression analyses in the OLSs model and the GWR model.

Table 5. VIF result of independent variables.

Variable	VIF [c]
Average Gross Domestic Product	1.257514
Population	1.750853
Total real estate investment	1.978460
Local financial income	4.085066
Percentage of third industry structure	2.468958
Density of the road	4.105955
Water area	1.875751

5.2.1. OLSs Regression Results

The OLSs regression model identifies significant relationships between ESBUA and its driving factors (Table 6). The model exhibits convincing explanatory power, with an adjusted R^2 of 0.75, indicating that 75% of the variance in BUA expansion is captured by the selected predictors. The overall model fit is statistically significant (F-test, $p < 0.001$). Among the seven independent variables, population, total real estate investment, density

of the road, and water area show statistically significant associations with the BUA at the 95% confidence level. However, average GDP, local financial income, and percentage of tertiary industry structure are not significant ($p > 0.05$), suggesting limited explanatory power in this model. The non-significant intercept (β = 55.177, $p = 0.230$) further suggests unobserved systematic bias.

Table 6. Summary results of the OLSs model.

ESBUA Model Coefficients—OLS		
Variables	**Coefficients**	***p*-Value**
Intercept	55.176536	0.230315
Average Gross Domestic Product	0.000917	0.232655
Population	−0.000005	0.000056 ***
Total real estate investment	0.000170	0.000000 ***
local financial income	3.722434	0.493152
Percentage of third industry structure	−0.956415	0.149769
Density of the road	−9.696236	0.030080 **
Water area	0.325214	0.035104 **
Prob(>F)	0.000000 *	
Adjusted R^2	0.7500000	

Note: * indicates the overall model is significant based on Prob(>F); ** = significant at 0.5% level *** = significant at 0.1% level.

To further explore possible reasons behind this unexplained variance, a global Moran's I statistic was calculated based on a Queen contiguity spatial weight matrix to assess spatial autocorrelation in BUA expansion from 1990 to 2018. The results (Moran's I = 0.213, z = 2.685, $p = 0.007$) confirm the presence of statistically significant positive spatial autocorrelation across the 52 county-level units in the GBA (Table 7). Therefore, the remaining 25% unexplained variability may be attributed to omitted spatial heterogeneity or non-linear interactions beyond the scope of this linear model. Therefore, this study will attempt to incorporate spatial heterogeneity into the model to better explain LUCC at the megacity region.

Table 7. ESBUA Moran's I.

Variable	**Moran's I**	***p*-Value**	**z**
ESBUA (1990–2018) (km^2)	0.213	0.007	2.685

5.2.2. GWR Regression Results

The GWR model demonstrates superior explanatory power compared to the OLSs model, with an adjusted R^2 of 0.92, up from 0.75 in the OLSs model. The residual sum of squares decreases from 9.50 to 5.50, and the AIC, serving as one of the effective information criteria to select and compare the best model [42], declines from 590.83 to 580.53, indicating GWR as a better model fit (Table 8). These results confirm that the GWR model effectively captures spatial variations in ESBUA drivers.

Table 8. Summary results of the OLSs and GWR model.

	OLS	**GWR**
Prob(>F)	0.0000 *	0.0000 *
Adjusted R^2	0.75	0.91
Residual sum of squares	9.50	5.50
AICc	590.8338	580.5323

Note: * indicates the overall model is significant based on Prob(>F).

Notably, some variables, such as GDP, which were not significant in the OLSs model, become significant in the GWR model, suggesting spatially varying influences. Infrastructure-related factors, including road density and water area, exhibit stronger significance, highlighting the role of spatial dependency in urban expansion. These findings reinforce the necessity of employing spatially adaptive models, such as GWR, to analyse LUCC drivers at the megacity region level, ensuring a more precise and localised understanding of urban growth processes (Table 9).

Table 9. Variables results of the OLSs and GWR model.

Variables	*p*-Value [a]	
	OLS	GWR
Intercept	0.2303	0.0000 ***
Average Gross Domestic Product	0.2326	0.0061 *
Population	0.0000 ***	0.0000 ***
Total real estate investment	0.0000 ***	0.0000 ***
local financial income	0.4546	0.4639
Percentage of third industry structure	0.0795	0.4967
Density of the road	0.0160 *	0.00 ***
Water area	0.0157 *	0.00 ***

Note: * = significant at the 1% level; *** = significant at 0.1% level; [a] Results of Monte Carlo test for spatial non-stationarity [51].

5.2.3. Coefficients Analysis

The regression coefficients derived from the GWR model results (see Appendix C) have been processed into coefficient distribution maps utilising the ArcGIS 10.0 tool. Figure 7 shows the spatial distribution of the intercept and all coefficients of the GWR model. The intercept term, or constant coefficients, establishes the fundamental level of urban LUCC across the study area in the absence of other influencing factors [52]. The intercept coefficient (β0) varies from −106.32 to 74, with a median of −18 instead of a constant (55.17) obtained from the global regression analysis. The outcome reveals a notable spatial variation in the constant coefficient, as illustrated in Figure 7a.

The coefficient estimates at a 95% significance level are presented to illustrate the spatial variation of the GWR model, with *p*-value of variables less than 0.05. Figure 7 depicts the spatial variation of coefficient estimations that may have influenced the increase in the GBA's BUA. A higher coefficient indicates that the effect of this variable is more significant in certain regions of the map [52]. In other words, areas represented by darker shading correspond to higher coefficient estimates.

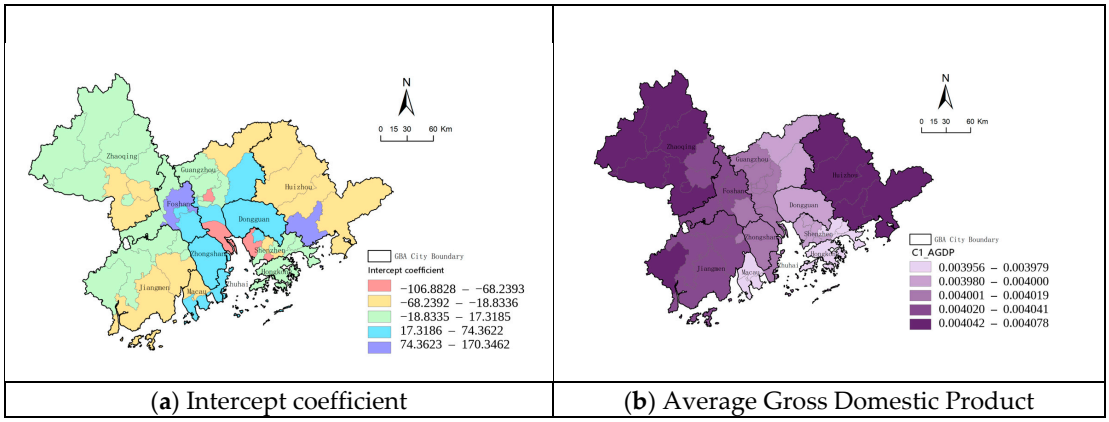

(**a**) Intercept coefficient (**b**) Average Gross Domestic Product

Figure 7. *Cont.*

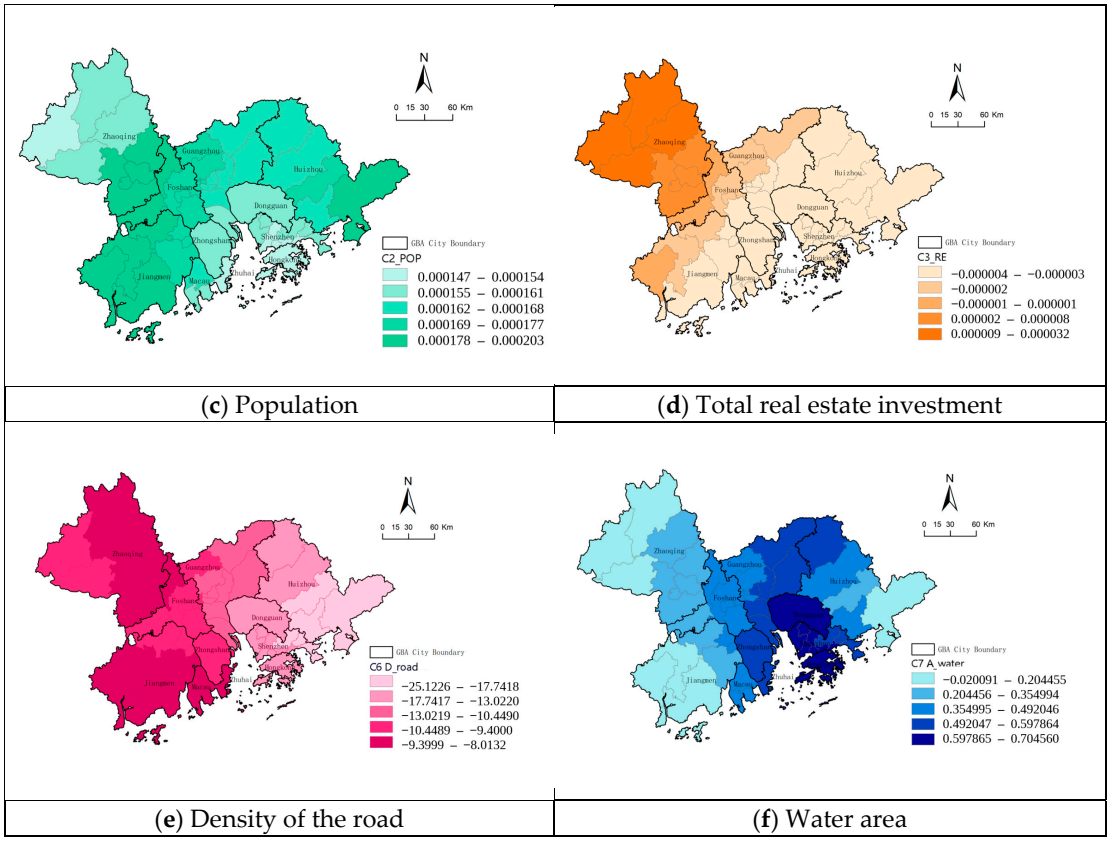

(**c**) Population (**d**) Total real estate investment

(**e**) Density of the road (**f**) Water area

Figure 7. Spatial distribution of the coefficient estimates of each independent variable.

The results of the GWR model show that the average gross domestic product, population, total real-estate investment, the density of the road, and water area are significantly relevant to the BUA expansion at the 95% significance level. In addition, local financial income and the percentage of the third industry structure are not obviously related to the BUA expansion.

(1) Population and Economy

In terms of economy, the coefficient (β0) of GBA per capita GDP to BUA expansion is 0.026915–0.027469 (Figure 7b), which means that if the annual per capita GDP increases at the rate of 1%, BUA expansion will increase by about 0.026915–0.027469%. The results of the OLSs model indicate that the per capita GDP of GBA has no significant impact on its growth, whereas the results of the GWR model reveal that per capita GDP has a statistically significant impact on BUA expansion. Therefore, the result of the GWR model indicates that economic growth promotes the expansion of the BUA. From the spatial dimension, the results of the GWR model exhibit a similar spatial distribution to that of the GDP. This study is more inclined to accept the results of the GWR model, given that some spatial differences in the OLSs model are not fully controlled, and thus, the estimation is biased.

In terms of population, the result of the GWR model shows that the coefficient (β1) of the population's impact on BUA expansion ranges between 0.00147 and 0.0020. The coefficient of the population indicates that for every 1.00% increase in per capita GDP, the expansion scale of the BUA will increase by 0.00147% to 0.002% (Figure 7c). Overall, the results of the GWR model are similar to those of OLSs, showing that the positive role of the population impacts BUA expansion. However, there are significant differences in the impact degree's spatial distribution of population variables in the GWR Model from the spatial dimension. The regression coefficients of the model are small in the southern coastal core cities (Macao, Hong Kong, Shenzhen, Zhuhai, Zhaoqing, and Dongguan).

That is, the impact of population growth on the BUA expansion is small. In the suburbs (Zhaoqing, Jiangmen, and Huizhou), population growth poses a more significant impact on the increase of construction areas.

(2) Real-estate investment

In terms of real-estate investment, the coefficient (β2) of the result of the GWR model shows that the impact on the BUA expansion ranges from −0.00004 to 0.00032 (Figure 7d). For every 1.00% increase in real estate investment, the scale of the BUA will increase by −0.00004–0.0032%. From the perspective of spatial distribution, it can be seen that there are spatial differences in the impact of real-estate investment on the BUA expansion. In the central cities of Guangdong, Hong Kong, and Macao, it has a negative impact and a positive impact on Suburban Cities (Zhaoqing, Jiangmen, and Foshan).

(3) Traffic construction

The coefficient (β5) of the traffic construction in the GWR model shows that the impact of traffic construction on BUA expansion ranges from −25 to −8.82 (Figure 7e), which indicates that the road network density has a negative correlation with BUA expansion. For every 1.00% increase in traffic network density, the scale of the BUA will be saved by 8.82–25%. From the spatial distribution, the impact intensity of the traffic construction scale decreases from north to south. It shows that the city's road network density has a negative impact on the BUA growth. This negative relationship may reflect an increase in land-use intensity, where areas with denser road networks tend to exhibit more efficient and compact urban development, thereby reducing the need for outward expansion of the BUA.

(4) Water Area

The water area is the most significant variable for the BUA expansion, and the coefficient (β6) of the water area in the model shows that the impact of the BUA distributes from −0.02 to 0.7 (Figure 7f), which indicates that the water area has a positive correlation with BUA expansion. For every 1.00% increase in the scale of water area in the study area, the scale of BUA will decrease by 0.02% to 0.7%. In terms of spatial distribution, the area with a higher positive value of the water area is located in the south of the Guangdong–Hong Kong–Macao Great Bay Area (GBA), especially in Shenzhen, Hong Kong, and Macao. This finding suggests that urban expansion in the study area often occurs near water areas, highlighting the marine resources and regional advantages of the GBA.

6. Discussion

There have been significant changes in land use and cover in the GBA from 1990 to 2018. Guangzhou, Shenzhen, Foshan, and Dongguan experienced the most remarkable urban expansion from 1990 to 2018, with average annual growth rates of 44.23 km^2, 22.64 km^2, 40.96 km^2, and 35.37 km^2, respectively. Meanwhile, Hong Kong and Macau experienced the slightest change in the same framework, with an average annual expansion of 3.44 and 0.21 km^2, respectively. Notably, LUCC in the GBA exhibited a distinctive cross-border, spatially networked expansion pattern even before the formal regional integration policies were introduced, extending BUA growth beyond core cities into decentralised urban nodes. Specifically, two prominent cross-border urban cores and one cross-administrative core emerged: one connecting Shenzhen and Hong Kong, and another linking Zhuhai and Macau. Moreover, an extensive cross-administrative connection developed between Guangzhou and Foshan.

The emergence of these three cores can be better understood by tracing their historical and institutional foundations. The Shenzhen–Hong Kong core reflects the long-standing

integration between export-processing manufacturing in Shenzhen and finance, logistics, and producer services in Hong Kong, reinforced by intensive cross-border commuting and successive waves of land development along major transport corridors such as highways, ports and, more recently, metro lines [53]. The Zhuhai–Macao core has been driven by Macao's tourism and gaming industries, the strategic development of the western bank of the Pearl River estuary, and port and infrastructure projects that facilitate the cross-border movement of visitors and workers [18]. The Guangzhou–Foshan core builds on decades of manufacturing specialisation in both cities, the gradual blurring of administrative boundaries, and the construction of an integrated transport network (metro lines and intercity rail) that has encouraged contiguous urban expansion [20,36]. Together, these processes have left a clear imprint on LUCC patterns in the form of cross-boundary BUA clusters, which are further reflected in the spatial configuration of the GWR coefficients.

On the other hand, although there is a clear trend towards integrated development, our study indicates that GBA urban expansion exhibits significant spatial imbalance issues. The local Moran's index result reveals the existence of a high–low agglomeration phenomenon in land use and cover within the GBA. It is evident that the challenges related to urban spatial expansion in the GBA mainly stem from an uncoordinated scale of urban space and the uneven spatial development among urban clusters. For example, certain adjacent cities such as Zhuhai and Zhongshan exhibited limited spatially interconnected urban expansion despite their geographical proximity. Meanwhile, peripheral cities such as Jiangmen and Zhaoqing exhibited minimal to no spatial integration with other GBA cities, reflecting broader regional disparities and fragmented urban networks.

In addition, historically, western countries occupied Hong Kong and Macau, which led to an advanced technology, economy and well-established land market in these regions prior to the 1990s. However, for mainland cities, China's critical land reform was initiated in 1990, which first allowed market-based urban land transfers in mainland cities. Economic growth and population increase generated a demand for additional land, while substantial investments in real estate and infrastructure facilitated the expansion of urban construction. However, following 1990, natural resource limitations significantly curtailed further growth of BUA in both Hong Kong and Macau. Macau's geographical constraints, which are surrounded by water with a total area of less than 40 square kilometres, leave minimal room for expansion. In contrast, Hong Kong's hilly terrain allows only 15% of the overall area to be developed as flat land. Furthermore, approximately 85% of its territory is unsuited for either urban construction or agricultural purposes. Additionally, stringent polices regulating land use/cover exacerbate this issue [54]. Consequently, Hong Kong experiences the lowest average growth rate of BUA.

The analysis is terminated in 2018, a year that both witnessed the GBA's formal endorsement and marked a structural policy breakpoint. In that year, the Ministry of Natural Resources introduced the national territorial–space control regime and the "three control lines" (ecological conservation redline, permanent basic farmland, and the urban development boundary), substantially tightening market- and locally led expansion and conversion of construction land. Accordingly, 1990–2018 can be delineated as a "market/land-concession–driven phase," with the post-2018 period entering a "policy-constrained phase," while the possibility of transitional bias and lagged effects is acknowledged. More broadly, this breakpoint signals a shift in the megacity-region context from a singular emphasis on urban growth to a triple-constraint paradigm—balancing growth, ecological sustainability, and food security.

The results of this research indicate that socio-economic factors, such as population, GDP, and real-estate investment, as well as natural factors, including road density and water area, have significant impacts on the growth of the BUA in various regions in the GBA

over the period from 1990 to 2018. The signs of their coefficients are generally consistent with our expectations, which align with the findings of other related studies. At a broader regional scale, however, pronounced spatial heterogeneity emerges due to differences in development stage, path-dependent historical trajectories, and environmental regulation and planning regimes.

Numerous studies highlight the importance of population and GDP in urban expansion [26]. Population growth and economic development are the internal drivers of urban development. The positive influence of population on BUA expansion is attributed to the heightened demand for urban land resulting from an increase in urban population. The analysis of the spatial distribution of GWR model coefficients reveals that both population and economic factors positively contribute to changes in the BUA. However, the degree of impact varies across different regions. Specifically, central cities in Guangdong, such as Hong Kong and Macao, experience a lesser impact compared to suburban areas. This discrepancy arises because Hong Kong and Macao are at different stages of urbanisation relative to mainland cities [55]. According to the three-stage theory of urbanisation development [11], a large number of infrastructure and supporting service facilities are required due to economic growth and population increases, particularly within the secondary and tertiary industries during the early phases of urbanisation. Consequently, this need promotes an increase in per capita BUA. Hong Kong and Macao have transitioned into later stages of urbanisation earlier than other cities within the GBA, which have undergone initial through medium-term stages since 1990. This is characterised by accelerated developmental phases in their respective processes of urbanisation. As a result, these nine cities maintain a higher rate of expansion regarding BUA compared to Hong Kong and Macao.

According to previous studies, land management and pricing have a significant impact on the expansion of urban land for construction in developing countries such as China [56]. This is mainly attributed to the substantial real-estate investment that contributes to an increase in BUA, such as the corresponding infrastructure [12,27,43]. However, this study finds that spatial differences regarding the influence of real estate investment on changes in BUA within the GBA. In cities in the early stages of urban development, characterised by low urbanisation rates and relatively low land prices, real estate investment has a significantly increasing effect on the growth of the BUA. For instance, in 2018, the average land price was RMB 7000 per square meter in Zhaoqing, RMB 9000 in Jiangmen, and RMB 13,000 in Foshan. Conversely, the areas with high urbanisation rates and elevated land prices have experienced restrained expansion of per capita BUA due to rising costs related to both increased property values and real-estate investments. These include Hong Kong at RMB 140,000 per square meter, Shenzhen at RMB 60,000, Macao at RMB 80,000, and Guangzhou at RMB 40,000. This phenomenon aligns with the principle of diminishing returns on land use. From a developer's perspective, higher land costs diminish profit margins for real estate developments, preferring higher density development strategies instead of investing in large areas of land. Consequently, this indicates that real-estate market development within the GBA is unevenly distributed, with more significant investments and faster expansions occurring in regions where both urbanisation levels and land prices are comparatively lower.

Both water area and transport factors significantly affect the changes in BUA, particularly regarding natural factors. Previous studies have found that marine rivers provide abundant natural resources for urban development, thereby promoting BUA expansion. However, these bodies of water may also pose a flood risk that negatively affects such expansions. The result of the GWR model reveals that the impact on the BUA varies between −0.02 and 0.7. Although there is spatial variation in the correlation between watershed area and BUA within the GBA, most coastal cities show a positive correlation.

This finding is consistent with the study by Hui and Li [2], which highlights how the advantageous location of the Bay Area and its economic relationship with maritime environments promote land expansion in coastal regions. Given the limited availability of land for outward growth, Shenzhen's proximity to the sea has led to an urban spatial expansion characterised by a tendency to spread towards marine areas. In addition, reclamation has emerged as a significant method for acquiring land in Hong Kong and Macao, where sea areas constitute 31.80% and 78.07% of total expansion areas in well-developed regions, respectively. These figures show considerably higher than those observed in other cities seeking to supply additional BUA, which creates a conflict between urban development and marine conservation.

The findings of this study demonstrate that the impacts of transport factors on the changes of the BUA across different areas are significant [57]. The signs of their coefficients are generally consistent with the expectations based on the related literature. While previous studies show that transportation development is a key driving force for spatial urban expansion, which plays a directional role in shaping spatial urban forms [18,58], the results of this study challenge this assumption in the context of highly urbanised regions. This implies that by 2018, the Greater Bay Area's fundamental core road network had already been established. Under these conditions, further increases in road density tend to support intensification and redevelopment (higher density, vertical expansion, land-use conversion) rather than horizontal expansion. This finding is consistent with historical patterns. This means in highly urbanised areas, a denser road network is generally associated with improved transport efficiency, better accessibility, and more intensive land use, reducing the demand for additional BUA. Therefore, for the Greater Bay Area megacity regions, intra-regional infrastructure connectivity should be encouraged, particularly along transportation corridors and at the peripheries of cities. At the same time, stronger central government coordination is needed to address inefficiencies arising from intercity competition and bargaining over infrastructure projects [18]. This is particularly relevant for large-scale transportation initiatives that extend beyond administrative boundaries, such as the Hong Kong-Zhuhai-Macao Bridge and the Shenzhen–Zhuhai Corridor, where conflicting local interests often lead to delays, cost overruns, and fragmented regional development.

Overall, from a broader regional perspective, the findings of the GWR coefficient reveal that spatial variations exist in the expansion of floor area across different regions within the Greater Bay Area, driven by distinct factors. This can be explained by differences in development stages, land prices, and local policy frameworks. From 1990 to 2018, core cities such as Guangzhou, Shenzhen, Hong Kong, and Macao entered a phase of mature or late-stage urbanisation, characterised by exceptionally high land prices and stringent planning controls. Within these cities, new population inflows and investment were more readily absorbed through redevelopment and vertical intensification, imposing structural constraints on further outward expansion of building floor area (BFA). By contrast, peripheral and suburban cities such as Jiangmen, Zhaoqing, and Huizhou retain substantial undeveloped land reserves and comparatively lower land prices. In these areas, population growth and property investment more directly translate into extensive BUA expansion. This contrast helps explain why property investment exhibits negative coefficients in some high-cost core cities yet positive coefficients in low-cost peripheral cities, and why identical drivers exert differing impacts on BUA expansion across distinct regions of the Greater Bay Area.

Beyond their implications for spatial structure, the observed LUCC patterns raise important sustainability concerns. The expansion of BUA has fragmented agricultural and forest land across the GBA, with potential consequences for regional food security, biodiversity conservation, and carbon storage. These pressures are compounded along

the coast, where land reclamation in cities such as Hong Kong, Macao, and Shenzhen has converted coastal wetlands and mudflats, increasing exposure to flooding and storm surges under conditions of sea-level rise and more frequent extreme weather events. Addressing these risks requires stronger forms of cross-jurisdictional spatial governance. In practical terms, this implies coordinated basic farmland protection and the designation of inter-city ecological corridors, stricter regulation of and ecological compensation for coastal reclamation, and the integration of LUCC indicators into the performance evaluation of GBA regional integration. Embedding such spatial-governance measures into the formal planning framework would help align regional economic ambitions with long-term ecological resilience.

7. Conclusions

This study examines LUCC in the Guangdong–Hong Kong–Macao Greater Bay Area (GBA) from 1990 to 2018, uncovering the spatial integration patterns preceding state-led formal institutional frameworks. The findings highlight two key aspects. First, even before the formal establishment of the GBA as a national strategic framework in 2018, the BUA in the region already exhibited cross-border spatial expansion, transcending administrative boundaries. Two prominent cross-border joint cores have formed (Shenzhen and Hong Kong; Zhuhai and Macau), along with one cross-administrative core (Guangzhou and Foshan). This was primarily driven by market forces and local government initiatives, rather than top-down policy directives. At the same time, the expansion of the BUA was not confined to core cities like Guangzhou and Shenzhen but also extended into decentralised urban nodes along transportation corridors, fostering a polycentric spatial network. This pattern was particularly evident in cities such as Dongguan, Foshan, and Zhuhai, where urbanisation spread across municipal borders, indicating an emerging functional integration of the megacity region even before policy formalisation. Second, despite the emergence of a cross-border urban network, the absence of a formal integration framework led to spatial imbalances and uncoordinated development patterns. Urban construction expansion varied considerably across cities, with rapid growth in mainland cities contrasting starkly with limited expansion in Hong Kong and Macao due to land constraints and governance differences. Moreover, uneven development intensified the fragmentation of agricultural and forest lands, alongside growing environmental pressures from coastal land reclamation. The impact of key driving factors—such as GDP growth, population increase, real estate investment, proximity to water, and road infrastructure development—varied significantly across different parts of the region, further exacerbating these spatial disparities.

The findings of this study have significant implications for regional planning and policymaking at both the national and regional levels. First, in the GBA case study, the observed BUA expansion in the GBA already exhibited a cross-border, spatially networked expansion pattern before formal regional integration policies. Thus, the definition and planning of megacity regions should recognise and leverage existing patterns of spatial and economic integration as indicated by LUCC, rather than solely relying on administrative boundaries. Second, these findings suggest that future land-use planning in the GBA requires coordinated cross-border spatial strategies, emphasising ecological protection, housing and industrial policies, and infrastructure and real estate investment. Ecological strategies should establish joint ecological corridors, protect green belts, and coordinate coastal land-use controls to mitigate fragmentation and reclamation pressures, safeguarding environmental sustainability. Housing and industrial land policies must optimise regional land-use efficiency, promoting cross-city housing initiatives and transport-oriented development to balance population density and alleviate socio-economic inequalities. Finally,

infrastructure and real-estate investments demand a unified regional approach, harmonising spatial planning and land policies across jurisdictions to prevent speculative and fragmented development, thereby facilitating interconnected and sustainable regional growth. Overall, the findings motivate an actionable governance checklist: systematic planning of cross-jurisdiction ecological corridors, rigid protection of permanent basic farmland, tighter entry standards and ecological compensation for coastal reclamation, and embedding key LUCC indicators in the GBA integration performance evaluation. These measures support more balanced spatial development under the triple constraint of growth, ecological sustainability, and food security.

This study presents several limitations. The remote sensing data utilised, obtained from the National GIS Centre, reveal discrepancies across different years due to the extended duration of the study period. Additionally, the study deliberately considered 2018—the formal designation year of the GBA—as a critical temporal threshold to isolate the effects of market-driven and local governmental forces from national strategic interventions. However, constraints related to data availability and consistency limited this research period to only 1990–2018. Future research would greatly benefit from extending the analysis beyond 2018 to explicitly incorporate and evaluate the impacts of national strategic planning and regional integration policies enacted thereafter. In terms of spatial land development strategies, while this study investigates the driving forces behind land-use changes, it has limitations for explaining continuous and dynamic LUCC driving factors across different periods. This limitation highlights the necessity for future research to explore these temporal dynamics in greater detail. Building on both the findings of this research and the existing literature, three key directions are proposed for future studies into LUCC in the GBA. First, the further exploration of agglomeration economies' influence on urban growth is necessary, particularly concerning the relationship between economic clustering and spatial development within the GBA. Second, conducting a cost–benefit analysis of land-use planning could facilitate an evaluation of land-use efficiency in this region. Third, the evaluation of the human–land linkage efficiency is essential for a better understanding of how population growth interacts with land expansion in the GBA.

Author Contributions: Conceptualisation, X.T. and C.Z.L.; methodology, X.T. and L.J.; software, X.T.; validation, X.T., R.W. and L.J.; formal analysis, X.T. and R.W.; investigation, X.T.; resources, J.X. and J.V.L.; data curation, X.T.; writing—original draft preparation, X.T.; writing—review and editing, J.X., R.W., J.V.L. and L.J.; visualisation, X.T.; supervision, J.X. and C.Z.L.; project administration, R.W.; funding acquisition, J.X. and C.Z.L. All authors have read and agreed to the published version of the manuscript.

Funding: This research was supported by the National Natural Science Foundation of China (NSFC) (Grant No. 52078302); the Guangdong Basic and Applied Basic Research Foundation (Grant No. 2024B1515020009); the Department of Education of Guangdong Province (Grant No. 2024ZDZX1012); the Shenzhen Science and Technology Innovation Commission (Grant No. JCYJ20220818102211024); the China Scholarship Council; and the PhD International Mobility Award from The Chinese University of Hong Kong.

Institutional Review Board Statement: Not applicable.

Informed Consent Statement: Not applicable.

Data Availability Statement: The original contributions presented in the study are included in the article; further inquiries can be directed to the corresponding author.

Conflicts of Interest: The authors declare no conflicts of interest.

Appendix A

Table A1. Land-use/cover data of each city in 1990 (Source: Author).

City	1990 (Area/km^2)					
	Grass	Agriculture	Forest	Build	Water	Unused
Guangzhou	107.8	2849.5	3183.0	615.3	433.8	4.9
Shenzhen	52.8	388.0	980.1	335.0	126.0	14.5
Zhuhai	9.4	667.7	521.3	80.1	211.3	17.4
Foshan	12.6	1602.7	908.7	345.0	923.3	3.3
Jiangmen	318.9	3092.0	4812.2	461.7	640.7	4.6
Zhaoqing	245.5	2640.1	11,288.1	245.7	478.8	0.0
Huizhou	268.9	2960.3	7327.5	399.1	322.4	3.7
Dongguan	90.8	856.5	858.6	356.1	279.6	1.9
Zhongshan	4.9	797.2	407.9	117.7	392.0	0.2
Hongkong	160.7	65.0	616.6	167.6	39.6	19.8
Macao	0.0	0.9	6.6	9.3	5.0	3.7

Table A2. Land-use/cover data of each city in 2000 (Source: Author).

City	2000 (Area/km^2)					
	Grass	Agriculture	Forest	Build	Water	Unused
Guangzhou	107.3	2585.5	3151.5	820.8	524.2	4.9
Shenzhen	32.5	300.9	871.7	587.1	104.2	0.0
Zhuhai	7.0	586.8	498.4	215.8	190.8	8.5
Foshan	12.5	1221.0	904.3	554.9	1099.7	3.3
Jiangmen	306.6	2854.9	4823.7	534.1	806.1	4.6
Zhaoqing	245.9	2562.7	11,284.2	283.4	522.1	0.0
Huizhou	265.6	2938.6	7320.5	420.3	335.3	1.5
Dongguan	83.0	680.4	755.4	634.1	288.8	1.9
Zhongshan	4.5	651.0	396.4	213.6	454.3	0.2
Hongkong	157.8	60.5	616.5	181.3	39.5	13.9
Macao	0.0	0.8	6.6	11.1	5.0	2.1

Table A3. Land-use/cover data of each city in 2010 (Source: Author).

City	2010 (Area/km^2)					
	Grass	Agriculture	Forest	Build	Water	Unused
Guangzhou	95.8	2134.0	3059.5	1357.2	553.8	9.7
Shenzhen	22.2	165.3	760.5	908.2	69.1	1.4
Zhuhai	6.7	296.5	480.3	320.4	418.7	20.5
Foshan	8.8	1317.2	860.9	1085.2	522.1	1.5
Jiangmen	274.4	2741.0	4775.2	694.4	847.0	3.9
Zhaoqing	238.3	2350.7	11,272.4	386.3	650.3	0.3
Huizhou	240.9	2722.8	7270.4	697.9	355.2	2.9
Dongguan	57.9	323.4	584.0	1190.8	291.9	0.5
Zhongshan	3.3	545.9	356.8	490.9	339.5	1.7
Hongkong	150.0	44.3	616.3	221.8	42.2	0.7
Macao	1.2	0.0	7.7	18.0	1.5	2.1

Table A4. Land-use/cover data of each city in 2018 (Source: Author).

City	2018 (Area/km^2)					
	Grass	**Agriculture**	**Forest**	**Build**	**Water**	**Unused**
Guangzhou	96.9	2079.2	3038.7	1470.0	523.1	2.1
Shenzhen	16.6	119.4	747.3	982.6	63.8	0.2
Zhuhai	15.2	402.4	474.6	402.0	251.5	1.5
Foshan	9.3	1249.3	842.4	1183.6	509.6	1.5
Jiangmen	311.4	2717.6	4691.2	798.3	816.8	0.8
Zhaoqing	303.0	2305.6	11,162.3	507.2	619.0	0.3
Huizhou	258.1	2637.7	7193.1	836.4	363.6	1.5
Dongguan	74.2	303.1	554.7	1244.0	272.0	0.1
Zhongshan	5.1	550.1	350.2	525.2	307.5	0.1
Hongkong	149.9	44.0	614.8	225.8	42.1	0.1
Macao	1.2	0.0	7.7	20.6	1.5	0.0

Appendix B

Table A5. Variable statistic data in the GWR model (Source: Author).

ID_City	ID_Districts	Average Gross Domestic Product	Total Real-Estate Investment	Population	Local Financial Income	Percentage of Third Industry Structure (%)	Density of the Road (km/km^2)	Water (km^2)
Macau	1	54.0641	8,205,520	675,400	24	96.123466	18.59892982	1.52347
Dongguan	2	9.8939	7,367,857	6,671,660	6.961	51.051457	3.110506073	272.041984
Foshan	3	15.8207	4,580,317	632,714	8.5471	59.303399	6.424836714	11.6702
	4	19.9182	1,306,494	248,112	6.3721	22.804844	1.001224412	46.5932
	5	9.8694	6,283,155	1,635,711	7.7422	43.376032	3.494233664	123.886
	6	18.5703	2,694,853	396,162	6.6467	25.677484	2.10706799	207.502
	7	11.8963	5,330,279	1,496,385	8.5008	42.446442	3.598818339	119.909

Table A5. *Cont.*

ID_City	ID_Districts	Average Gross Domestic Product	Total Real-Estate Investment	Population	Local Financial Income	Percentage of Third Industry Structure (%)	Density of the Road (km/km^2)	Water (km^2)
Guangzhou	8	7.4239	1,909,690	1,353,103	11.4836	81.293928	4.482480061	56.4584
	9	6.4641	1,003,901	423,148	9.7819	50.721160	0.956406938	31.2089
	10	11.8923	2,159,830	760,604	8.7486	63.880700	3.535748936	95.086496
	11	11.2103	1,622,431	674,278	11.1563	84.856775	8.86501493	13.231
	12	12.5305	3,619,981	1,192,356	9.335	44.913521	2.643845997	69.981296
	13	31.4288	3,190,702	809,460	11.0644	40.424971	3.115858231	23.11
	14	12.7432	2,109,332	349,887	9.6448	77.726016	7.842591409	6.06268
	15	19.7523	2,543,749	501,345	9.9439	37.662638	1.693742415	159.975008
	16	26.7604	2,713,582	1,277,937	12.7325	92.953280	8.03132929	4.42162
	17	28.0156	275,136	897,891	10.9165	98.184048	16.22569641	3.08964
	18	9.3025	5,870,989	725,398	9.7587	58.133703	1.247403448	60.4422
Huizhou	19	6.0714	1,019,288	634,941	6.7756	41.815808	0.545555125	113.126
	20	8.6100	2,981,618	952,176	8.0456	50.596274	1.024747431	133.29
	21	6.6717	1,471,256	574,745	7.3058	55.744505	0.497065686	71.2586
	22	14.8609	3,844,590	566,878	7.6828	28.134434	1.21141054	20.3776
	23	5.5476	522,665	174,596	7.1179	50.623362	0.317225001	25.5106
Jiangmen	24	3.9218	594,527	202,318	6.0984	59.749021	0.600507148	76.363904
	25	6.9751	694,047	277,870	6.4793	41.986338	0.966710256	43.7146
	26	7.0985	763,450	150,821	6.8014	34.938610	4.155105758	28.7744
	27	5.2429	449,954	417,749	6.6415	41.520449	0.799513348	84.0606
	28	8.8727	1,191,921	420,503	7.5975	60.650186	3.864034533	42.8877
	29	4.5394	726,892	531,906	6.5053	30.078324	0.681773769	337.836
	30	7.7659	1,330,197	470,181	7.4514	36.705374	1.260784123	203.194
Shenzhen	31	11.2761	3,806,755	2,252,703	8.0044	48.999328	6.443715813	25.175
	32	25.1542	2,659,563	2,015,689	13.1381	94.022514	13.83182931	3.15684
	33	15.0694	1,287,625	182,063	7.7276	35.883010	4.011256925	4.10329
	34	18.6509	5,691,425	1,660,329	11.32723589	31.654492	3.582631893	12.4034
	35	14.6609	3,992,874	1,228,667	7.9495	40.084514	4.669296663	2.45936
	36	21.8054	1,242,977	849,472	12.8932	96.319040	7.838635809	5.30963
	37	34.3936	5,795,466	1,475,727	13.8218	59.214346	10.5205929	5.03208
	38	16.0507	1,410,703	309,864	8.3389	35.626310	2.586781677	4.50806
	39	25.5265	407,767	137,006	11.3414	85.969586	4.9242857	1.68607
Hongkong	40	31.5698	88,205,520	3,979,000	18.7248	92.132457	8.06232544	42.1082

Table A5. *Cont.*

ID_City	ID_Districts	Average Gross Domestic Product	Total Real-Estate Investment	Population	Local Financial Income	Percentage of Third Industry Structure (%)	Density of the Road (km/km^2)	Water (km^2)
Zhaoqing	41	4.1039	53,632	195,518	6.6696	48.012217	0.178690486	51.8438
	42	6.3852	567,495	102,917	6.2453	37.663177	0.450598137	132.281
	43	10.2430	755,260	259,791	7.9464	73.750206	2.355277637	21.3513
	44	3.9373	26,946	208,030	5.799	39.470573	0.15446998	79.3812
	45	5.4378	566,058	482,022	7.2448	40.297467	0.402944046	147.328
	46	3.5929	171,116	246,008	6.2759	43.278004	0.201220677	15.1665
	47	2.8757	267,314	394,751	6.3572	48.725101	0.286484185	34.2852
	48	9.7076	1,070,592	363,972	6.748118887	42.420067	0.429413127	137.374
Zhongshan	49	11.0585	6,972,228	2,129,894	7.403	49.298958	2.702047519	307.456
Zhuhai	50	8.1679	1,149,466	180,452	7.7497	35.453466	1.998500965	119.377
	51	21.3982	1,076,158	222,521	8.0326	25.764832	2.185287208	101.621
	52	17.9270	5,645,296	756,743	8.994	59.529312	4.55550738	30.5232

Appendix C

Table A6. The regression results of the GWR model (Source: Author).

ID_City	ID_Districts	Observed	Cond	LocalR^2	Predicted	Intercept
Macau	1	20.592699	5.286830	0.896456	−53.769541	37.983487
Dongguan	2	1243.959961	5.557242	0.946876	1203.401254	55.855030
Foshan	3	120.751999	5.676211	0.895047	76.434921	37.263981
	4	97.751602	5.367596	0.867641	80.433119	30.315930
	5	495.372986	5.694610	0.892249	325.026751	34.639685
	6	139.906998	5.635170	0.880644	153.815450	20.664056
	7	329.816010	5.619532	0.905360	294.472041	42.107992
Guangzhou	8	242.294998	5.686652	0.919960	243.254683	39.291964
	9	90.168800	5.434583	0.946548	110.421401	36.229768
	10	213.906006	5.658453	0.925245	172.692931	45.265634
	11	64.144302	5.697467	0.919912	61.890357	42.947186
	12	225.791000	5.665084	0.908647	236.679470	30.729155
	13	158.223999	5.629816	0.934896	143.399971	45.100669
	14	54.591599	5.716017	0.910901	14.769374	40.379679
	15	101.695999	5.566012	0.927327	186.343473	45.883178
	16	93.932701	5.685736	0.924465	162.172016	43.095890
	17	27.261600	5.712697	0.916009	23.838235	41.117560
	18	198.033005	5.578977	0.949517	161.582453	47.135755

Table A6. *Cont.*

ID_City	ID_Districts	Observed	Cond	LocalR^2	Predicted	Intercept
Huizhou	19	186.145004	6.025300	0.955397	204.978651	60.253205
	20	226.033997	6.134507	0.950025	248.354208	74.869196
	21	129.740997	6.288265	0.924542	176.899313	92.592665
	22	247.380005	5.980389	0.945454	140.869675	79.016769
	23	47.109001	5.860120	0.958125	79.223829	42.329382
Jiangmen	24	97.019096	4.750765	0.863373	85.760869	38.423161
	25	100.449997	5.319083	0.873886	91.717826	37.927297
	26	39.960201	5.398390	0.895098	37.892018	42.799039
	27	119.345001	4.906290	0.864752	130.863792	40.026833
	28	101.955002	5.448811	0.892042	90.257656	41.922615
	29	186.692001	4.840259	0.860486	209.204426	49.758731
	30	152.893997	5.226514	0.883420	181.119910	44.126737
Shenzhen	31	244.518997	5.455105	0.938119	317.380582	53.150051
	32	50.596802	5.406413	0.935351	157.479618	58.560280
	33	87.496002	5.494013	0.942888	25.741159	56.910898
	34	255.815002	5.691851	0.940591	252.502614	73.247007
	35	122.344002	5.478143	0.941541	166.077833	60.215675
	36	29.051300	5.470384	0.937763	70.373937	63.817412
	37	105.283997	5.393970	0.934063	118.367707	54.021197
	38	70.001297	5.752563	0.942046	73.115346	74.677835
	39	17.449699	5.588850	0.939046	7.490492	69.858151
Hongkong	40	225.824005	5.353256	0.926532	235.509174	59.266996
Zhaoqing	41	45.428600	6.141561	0.923214	42.722509	4.400842
	42	43.733398	5.392580	0.871810	69.843398	11.962266
	43	52.389000	5.278993	0.871963	51.197913	11.988287
	44	36.764599	7.513590	0.929248	43.079745	2.094082
	45	103.787003	5.268618	0.871811	140.973189	12.374601
	46	38.008598	5.686279	0.925745	41.666106	−2.928398
	47	68.540497	6.843967	0.934481	69.472349	−4.129022
	48	118.582001	5.311009	0.879334	120.993456	4.875403
Zhongshan	49	525.215027	5.444828	0.910999	489.764592	41.958740
Zhuhai	50	81.589401	5.250404	0.887507	102.106645	42.636569
	51	161.414993	5.188905	0.873892	100.290830	44.832094
	52	159.009995	5.303631	0.902377	107.270396	38.249503

Table A7. The regression coefficients of the GWR model (Source: Author).

ID_City	ID_Districts	C1_AGDP	C2_POP	C3_RE	C4_Income	C5_I3	C6 D_Road	C7 A_Water	Residual	StdError	StdResid
Macau	1	0.004003	0.000151	−0.00000393	5.4125	−0.8564	−8.7406	0.5791	74.3622	23.1516	3.2120
Dongguan	2	0.003992	0.000158	−0.00000402	2.7623	−0.7571	−14.0451	0.6100	40.5587	16.9090	2.3986
Foshan	3	0.004022	0.000176	−0.00000299	0.9239	−0.8052	−9.8636	0.4095	44.3171	50.9480	0.8698
	4	0.004037	0.000191	−0.00000061	0.6537	−0.9033	−9.4000	0.2767	17.3185	49.2549	0.3516
	5	0.004023	0.000177	−0.00000250	0.6930	−0.8060	−9.7302	0.4030	170.3462	50.0697	3.4022
	6	0.004029	0.000181	0.00000087	0.0553	−0.8272	−8.9653	0.3754	−13.9085	39.4225	−0.3528
	7	0.004017	0.000171	0.00000380	1.6200	−0.7961	−10.1481	0.4467	35.3440	51.9507	0.6803
Guangzhou	8	0.004013	0.000170	−0.00000324	0.5544	−0.7348	−10.4490	0.4862	−0.9597	51.4114	−0.0187
	9	0.004000	0.000165	−0.00000321	0.0319	−0.6809	−10.6788	0.5720	−20.2526	45.4043	−0.4461
	10	0.004009	0.000165	−0.00000398	1.6142	−0.7513	−11.0400	0.5190	41.2131	52.3807	0.7868
	11	0.004012	0.000168	−0.00000374	1.1287	−0.7506	−10.7053	0.4920	2.2539	50.9153	0.0443
	12	0.004017	0.000173	−0.00000179	0.1111	−0.7464	−9.7042	0.4547	−10.8885	50.7112	−0.2147
	13	0.004006	0.000165	0.00000387	1.0102	−0.7189	−11.3492	0.5388	14.8240	50.3835	0.2942
	14	0.004016	0.000171	0.00000344	0.9497	−0.7660	−10.3290	0.4617	39.8222	50.9512	0.7816
	15	0.004005	0.000161	0.00000408	2.5891	−0.7673	−11.2110	0.5570	−84.6475	48.9793	−1.7282
	16	0.004010	0.000167	−0.00000372	0.9773	−0.7373	−10.8451	0.5044	−68.2393	50.4208	−1.3534
	17	0.004014	0.000170	−0.00000352	0.9077	−0.7532	−10.4927	0.4773	3.4234	33.5265	0.1021
	18	0.003996	0.000162	−0.00000397	1.0181	−0.7045	−12.3386	0.5860	36.4506	49.6029	0.7348
Huizhou	19	0.004044	0.000166	−0.00000407	1.9671	−0.7989	−16.7759	0.4629	−18.8336	44.3945	−0.4242
	20	0.004045	0.000170	−0.00000411	3.2290	−0.8825	−20.1186	0.3353	−22.3202	40.7924	−0.5472
	21	0.004045	0.000182	−0.00000424	5.0451	−1.0865	−25.1226	−0.0101	−47.1583	42.0045	−1.1227
	22	0.004042	0.000164	−0.00000398	4.5475	−0.9043	−20.0327	0.4271	106.5103	47.1326	2.2598
	23	0.004077	0.000165	−0.00000380	0.6151	−0.7347	−13.0220	0.5591	−32.1148	41.5798	−0.7724
Jiangmen	24	0.004051	0.000203	−0.00000025	1.2285	−0.9900	−9.0621	0.1566	11.2582	43.5564	0.2585
	25	0.004032	0.000186	−0.00000273	1.3253	−0.8883	−9.4542	0.2984	8.7322	49.0095	0.1782
	26	0.004019	0.000171	−0.00000405	2.5204	−0.8374	−9.4864	0.4126	2.0682	50.8721	0.0407
	27	0.004041	0.000197	−0.00000230	1.5831	−0.9562	−9.1237	−0.0013	−11.5188	48.3418	−0.2383
	28	0.004022	0.000174	−0.00000382	1.9647	−0.8382	−9.6343	−0.0201	11.6973	51.7728	0.2259
	29	0.004034	0.000187	0.00000421	3.3246	−0.9613	−8.1985	−0.0125	−22.5124	23.0150	−0.9782
	30	0.004023	0.000174	0.00000411	2.8738	−0.8728	−8.9985	0.3550	−28.2259	48.0663	−0.5872
Shenzhen	31	0.003993	0.000155	0.00000395	3.8154	−0.7878	−13.3020	0.6363	−72.8616	49.6988	−1.4661
	32	0.003986	0.000151	−0.00000382	4.9680	−0.8332	−14.3357	0.6679	−106.8828	42.3493	−2.5238
	33	0.003990	0.000156	−0.00000395	3.6243	−0.7850	−14.2127	0.6302	61.7548	50.7946	1.2158
	34	0.003977	0.000155	−0.00000382	5.2892	−0.8865	−17.7418	0.5917	3.3124	46.9215	0.0706
	35	0.003987	0.000154	−0.00000389	4.2620	−0.8117	−14.8943	0.6417	−43.7338	50.4356	−0.8671
	36	0.003983	0.000152	−0.00000380	5.1046	−0.8485	−15.4698	0.6573	−41.3226	51.0684	−0.8092
	37	0.003990	0.000152	−0.00000386	4.6391	−0.8160	−13.4153	0.6615	−13.0837	49.8230	−0.2626
	38	0.003976	0.000157	−0.00000385	5.1343	−0.8889	−18.2357	0.5630	−3.1140	49.0607	−0.0635
	39	0.003979	0.000153	−0.00000380	5.3346	−0.8743	−16.8240	0.6293	9.9592	50.2426	0.1982

Table A7. *Cont.*

ID_City	ID_Districts	C1_AGDP	C2_POP	C3_RE	C4_Income	C5_I3	C6 D_Road	C7 A_Water	Residual	StdError	StdResid
Hongkong	40	0.003958	0.000147	−0.00000370	6.0704	−0.8738	−14.0754	0.7046	−9.6852	3.4559	−2.8025
Zhaoqing	41	0.004066	0.000158	−0.00002845	−1.3464	−0.9703	−9.8565	0.1483	2.7061	44.2747	0.0611
	42	0.004040	0.000187	−0.00000566	−0.1886	−0.8998	−8.7548	0.2978	−26.1100	47.9965	−0.5440
	43	0.004045	0.000189	−0.00000760	−0.2790	−0.9333	−8.9611	0.2527	1.1911	48.0835	0.0248
	44	0.004078	0.000151	−0.00003228	−1.8038	−0.9224	−9.6078	0.1296	−6.3151	38.7651	−0.1629
	45	0.004046	0.000190	0.00000768	−0.2807	−0.9368	−9.0011	−0.0201	−37.1862	46.9568	−0.7919
	46	0.004049	0.000157	0.00002502	−0.5976	−0.9306	−8.9865	−0.0200	−3.6575	40.7713	−0.0897
	47	0.004061	0.000157	0.00002667	−0.5689	−0.9552	−8.9574	−0.1045	−0.9319	37.2810	−0.0250
	48	0.004038	0.000181	0.00000788	−0.3380	−0.8789	−8.3576	0.3295	−2.4115	48.5576	−0.0497
Zhongshan	49	0.004010	0.000161	−0.00000411	3.3080	−0.8088	−9.8708	0.5198	35.4504	37.6895	0.9406
Zhuhai	50	0.003967	0.000163	−0.00000419	4.1354	−0.8637	−8.5741	0.4361	−20.5172	49.8890	−0.4113
	51	0.003970	0.000160	−0.00000420	5.0172	−0.8923	−8.0132	0.4121	61.1242	48.8761	1.2506
	52	0.004010	0.000151	−0.00000392	5.2563	−0.8467	−9.1387	0.5979	51.7396	50.2377	1.0299

References

1. Xu, J.; Yeh, A.G. *Governance and Planning of Mega-City Regions: An International Comparative Perspective*; Routledge: Abingdon, UK, 2011.
2. Hui, E.C.; Li, X.; Chen, T.; Lang, W. Deciphering the spatial structure of China's megacity region: A new bay area—The Guangdong-Hong Kong-Macao Greater Bay Area in the making. *Cities* **2020**, *105*, 102168. [CrossRef]
3. Harrison, J.; Gu, H. Planning megaregional futures: Spatial imaginaries and megaregion formation in China. In *Planning Regional Futures*; Routledge: Oxfordshire, UK, 2021; pp. 148–171.
4. Gaur, S.; Singh, R. A comprehensive review on land use/land cover (LULC) change modeling for urban development: Current status and future prospects. *Sustainability* **2023**, *15*, 903. [CrossRef]
5. Harrison, J.; Gu, H. Arguing with megaregions: Learning from China's chéngshì qún. *Trans. Plan. Urban Res.* **2023**, *2*, 53–70. [CrossRef]
6. Cheng, E.W.; Tong, K.-L. Variegated city-region governance: Centralised design, localised implementation and asymmetric integration in China's Greater Bay Area. *Territ. Politics Gov.* **2025**, *13*, 716–736. [CrossRef]
7. United Nations Population Fund (UNFPA). *World Population Dashboard*; UNFPA: New York, NY, USA, 2019.
8. United Nations. *Population*; United Nations: New York, NY, USA, 2019.
9. Lv, T.; Wang, L.; Xie, H.; Zhang, X.; Zhang, Y. Exploring the global research trends of land use planning based on a bibliometric analysis: Current status and future prospects. *Land* **2021**, *10*, 304. [CrossRef]
10. Mu, F.; Zhang, Z. A comparative study of urban expansion on Hong Kong and Macao special administrative region in the past three decades. In Proceedings of the 2008 International Workshop on Earth Observation and Remote Sensing Applications, Beijing, China, 30 June–2 July 2008; pp. 1–6.
11. Fang, C.; Yu, D. Urban agglomeration: An evolving concept of an emerging phenomenon. *Landsc. Urban Plan.* **2017**, *162*, 126–136. [CrossRef]
12. Tang, X.; Li, C.Z.; Jiang, L.; Lai, X.; Zhang, L. A Spatial Autocorrelation Analysis for Land Use Change in the Guangdong-Hong Kong-Macao Greater Bay Area. In Proceedings of the International Symposium on Advancement of Construction Management and Real Estate, Beijing, China, 20–22 November 2021; Springer: Singapore, 2021; pp. 847–858.
13. Xie, Q.; Ghanbari Parsa, A.; Redding, B. The emergence of the urban land market in China: Evolution, structure, constraints and perspectives. *Urban Stud.* **2002**, *39*, 1375–1398. [CrossRef]
14. Gottmann, J. Megalopolis or the urbanization of the northeastern seaboard. *Econ. Geogr.* **1957**, *33*, 189–200. [CrossRef]
15. Hall, P.G.; Pain, K. *The Polycentric Metropolis: Learning from Mega-City Regions in Europe*; Routledge: Oxfordshire, UK, 2006.
16. Harrison, J.; Hoyler, M. *Megaregions: Globalization's New Urban Form?* Edward Elgar Publishing: Cheltenham, UK, 2015.
17. Scott, A.J. *Global City-Regions: Trends, Theory, Policy*; OUP Oxford: Oxfordshire, UK, 2001.
18. Xu, J.; Yeh, A.G. Interjurisdictional cooperation through bargaining: The case of the Guangzhou–Zhuhai railway in the Pearl River Delta, China. *China Q.* **2013**, *213*, 130–151. [CrossRef]
19. Wu, R.; Li, Z.; Wang, S. The varying driving forces of urban land expansion in China: Insights from a spatial-temporal analysis. *Sci. Total Environ.* **2021**, *766*, 142591. [CrossRef]
20. Constitutional and Mainland Affairs Bureau. *Guangdong-Hong Kong-Macao Greater Bay Area—Outline Development Plan*; Government of the Hong Kong SAR: Hong Kong, China, 2021.
21. Association of Bay Area Governments; Metropolitan Transportation Commission. *Plan Bay Area 2050*; Metropolitan Transportation Commission: San Francisco, CA, USA, 2021.
22. Hua, W.; Chen, H.; Sun, S.; Zhou, L. Assessing climatic impacts of future land use and land cover change projected with the CanESM2 model. *Int. J. Climatol.* **2015**, *35*, 3661–3675. [CrossRef]
23. Geist, H.; McConnell, W.; Lambin, E.F.; Moran, E.; Alves, D.; Rudel, T. Causes and trajectories of land-use/cover change. In *Land-Use and Land-Cover Change: Local Processes and Global Impacts*; Springer: Berlin/Heidelberg, Germany, 2006; pp. 41–70.
24. Bella, K.P.; Irwin, E.G. Spatially explicit micro-level modelling of land use change at the rural–urban interface. *Agric. Econ.* **2002**, *27*, 217–232. [CrossRef]
25. Briassoulis, H. *Analysis of Land Use Change: Theoretical and Modeling Approaches*; Regional Research Institute, West Virginia University: Morgantown, WV, USA, 2000.
26. Zhou, Y.; Zhong, Z.; Cheng, G. Cultivated land loss and construction land expansion in China: Evidence from national land surveys in 1996, 2009 and 2019. *Land Use Policy* **2023**, *125*, 106496. [CrossRef]
27. Ran, T. The issue of land in China's transition and urbanization. In *China's Great Urbanization*; Routledge: Oxfordshire, UK, 2016; pp. 139–163.
28. Lloyd, C.B. *Growing Up Global: The Changing Transitions to Adulthood in Developing Countries*; National Academies Press: Washington, DC, USA, 2005.
29. Chen, J.; Chang, K.-T.; Karacsonyi, D.; Zhang, X. Comparing urban land expansion and its driving factors in Shenzhen and Dongguan, China. *Habitat Int.* **2014**, *43*, 61–71. [CrossRef]

30. Gong, P.; Li, X.; Wang, J.; Bai, Y.; Chen, B.; Hu, T.; Liu, X.; Xu, B.; Yang, J.; Zhang, W. Annual maps of global artificial impervious area (GAIA) between 1985 and 2018. *Remote Sens. Environ.* **2020**, *236*, 111510. [CrossRef]
31. National Bureau of Statistics. *China Statistical Yearbook*; National Bureau of Statistics: Beijing, China, 2019.
32. National Bureau of Statistics of China. *China City Statistical Yearbook*; China Statistics Press: Beijing, China, 2018.
33. Guangdong Provincial Bureau of Statistics. *Guangdong Statistical Yearbook*; China Statistics Press: Beijing, China, 2018.
34. Statistics and Census Service (DSEC), Government of the Macao Special Administrative Region. *Macao Statistical Yearbook*; Statistics and Census Service: Macao, China, 2018.
35. Census and Statistics Department, Government of the Hong Kong Special Administrative Region; Census and Statistics Department. *Hong Kong Statistical Yearbook*; Census and Statistics Department: Hong Kong, China, 2018.
36. Hong, K.-R.; Qiu, L.-S.; Yang, D.-X.; Jiang, M. Spatio-temporal evolution and correlation analysis of urban land use patterns and air quality in pearl river delta, China. *Front. Environ. Sci.* **2021**, *9*, 698383. [CrossRef]
37. Anselin, L. Local indicators of spatial association—LISA. *Geogr. Anal.* **1995**, *27*, 93–115. [CrossRef]
38. Pap, A. Logic and the synthetic a priori. *Philos. Phenomenol. Res.* **1950**, *10*, 500–514. [CrossRef]
39. Frantál, B.; Greer-Wootten, B.; Klusáček, P.; Krejčí, T.; Kunc, J.; Martinát, S. Exploring spatial patterns of urban brownfields regeneration: The case of Brno, Czech Republic. *Cities* **2015**, *44*, 9–18. [CrossRef]
40. Akinwande, M.O.; Dikko, H.G.; Samson, A. Variance inflation factor: As a condition for the inclusion of suppressor variable (s) in regression analysis. *Open J. Stat.* **2015**, *5*, 754. [CrossRef]
41. Getis, A. Cliff, ad and ord, jk 1973: Spatial autocorrelation. london: Pion. *Prog. Hum. Geogr.* **1995**, *19*, 245–249. [CrossRef]
42. Fotheringham, A.S.; Brunsdon, C.; Charlton, M. Geographically weighted regression. *Sage Handb. Spat. Anal.* **2009**, *1*, 243–254.
43. Tyzhnenko, A.G.; Ryeznik, Y.V. Ordinary Least Squares: The Adequacy of Linear Regression Solutions Under Multicollinearity and Without It. *Probl. Econ.* **2019**, *1*, 217–227. [CrossRef]
44. Gao, J.; Wei, Y.D.; Chen, W.; Chen, J. Economic transition and urban land expansion in Provincial China. *Habitat Int.* **2014**, *44*, 461–473. [CrossRef]
45. Hou, M.; Ge, J.; Gao, J.; Meng, B.; Li, Y.; Yin, J.; Liu, J.; Feng, Q.; Liang, T. Ecological risk assessment and impact factor analysis of alpine wetland ecosystem based on LUCC and boosted regression tree on the Zoige Plateau, China. *Remote Sens.* **2020**, *12*, 368. [CrossRef]
46. Forman, R.T.; Alexander, L.E. Roads and their major ecological effects. *Annu. Rev. Ecol. Syst.* **1998**, *29*, 207–231. [CrossRef]
47. Ibisch, P.L.; Hoffmann, M.T.; Kreft, S.; Pe'er, G.; Kati, V.; Biber-Freudenberger, L.; DellaSala, D.A.; Vale, M.M.; Hobson, P.R.; Selva, N. A global map of roadless areas and their conservation status. *Science* **2016**, *354*, 1423–1427. [CrossRef]
48. Recanatesi, F.; Petroselli, A. Land cover change and flood risk in a peri-urban environment of the metropolitan area of Rome (Italy). *Water Resour. Manag.* **2020**, *34*, 4399–4413. [CrossRef]
49. Pattison, I.; Lane, S.N. The link between land-use management and fluvial flood risk: A chaotic conception? *Prog. Phys. Geogr.* **2012**, *36*, 72–92. [CrossRef]
50. Cao, X.; Liu, Y.; Li, T.; Liao, W. Analysis of spatial pattern evolution and influencing factors of regional land use efficiency in China based on ESDA-GWR. *Sci. Rep.* **2019**, *9*, 520. [CrossRef]
51. Fotheringham, A.S. Analysing numerical spatial data. In *Methods in Human Geography*; Routledge: Oxfordshire, UK, 2013; pp. 191–206.
52. Huang, Y.; Leung, Y. Analysing regional industrialisation in Jiangsu province using geographically weighted regression. *J. Geogr. Syst.* **2002**, *4*, 233–249. [CrossRef]
53. Statistics Bureau of Shenzhen Municipality. *Shenzhen Statistical Yearbook*; Statistics Bureau of Shenzhen Municipality: Shenzhen, China, 2019.
54. Wang, C.; Wu, J.; Li, M.; Huang, X.; Lei, C.; Wang, H. Evaluation of spatial conflicts of land use and its driving factors in arid and semiarid regions: A case study of Xinjiang, China. *Ecol. Indic.* **2024**, *166*, 112483. [CrossRef]
55. Dang, V.Q.; Kwan, F.; Lam, A.I. Guangdong–Hong Kong–Macao Greater Bay Area (GBA): Economic progress, diversification, and convergence. *J. Asia Pac. Econ.* **2023**, *30*, 158–189. [CrossRef]
56. Zhao, P. Managing urban growth in a transforming China: Evidence from Beijing. *Land Use Policy* **2011**, *28*, 96–109. [CrossRef]
57. Zhao, P. Sustainable urban expansion and transportation in a growing megacity: Consequences of urban sprawl for mobility on the urban fringe of Beijing. *Habitat Int.* **2010**, *34*, 236–243. [CrossRef]
58. Chen, J.; Dowman, I.; Li, S.; Li, Z.; Madden, M.; Mills, J.; Paparoditis, N.; Rottensteiner, F.; Sester, M.; Toth, C. Information from imagery: ISPRS scientific vision and research agenda. *ISPRS J. Photogramm. Remote Sens.* **2016**, *115*, 3–21. [CrossRef]